J. Fluid Mech. (1997), *vol.* 347, *pp.* 315–346. Printed in the United Kingdom

Influence of mean loading on noise generated by the interaction of gusts with a flat-plate cascade: upstream radiation

By N. PEAKE[1] AND E. J. KERSCHEN[2]

[1]Department of Applied Mathematics and Theoretical Physics, University of Cambridge, Silver Street, Cambridge CB3 9EW, UK

[2]Department of Aerospace and Mechanical Engineering, University of Arizona, Tucson, AZ 85721, USA

(Received 14 August 1996 and in revised form 20 May 1997)

The sound generated by the interaction between convected vortical and entropic disturbances and a blade row is a significant component of the total noise emitted by a modern aeroengine, and the blade geometry has an important effect on this process. As a first step in the development of a general prediction scheme, we model in this paper just the action of the blade mean loading by treating the blades as flat plates aligned at a non-zero incidence angle, δ, to the oncoming stream, and consider harmonic components of the incident field with reduced frequency k. We then use asymptotic analysis in the realistic limit $k \gg 1$, $\delta \ll 1$ with $k\delta = O(1)$ to make a consistent asymptotic expansion of the compressible Euler equations. The flow is seen to consist of inner regions around each leading edge, in which sound is generated by the local gust–airfoil and gust–flow interactions, and an outer region in which both the incident gust is distorted according to rapid distortion theory and the out-going sound is refracted by the non-uniform mean flow. The complicated multiple interactions between the sound and the cascade are included to the appropriate asymptotic order, and analytical expressions for the forward radiation are derived. It is seen that even a relatively small value of δ can have a significant effect, thanks to both the $O(\delta k^{1/2})$ change in the amplitudes and the $O(k\delta)$ change in the phases of the various radiation components, corresponding to the additional source mechanisms associated with the flow distortion around each leading edge and the effects of propagation through the non-uniform flow, respectively. Further work will extend this analysis to include the effects of camber and thickness.

1. Introduction

The continued environmental pressure to reduce community noise levels around large airports, coupled with the development of increasingly advanced aeroengines, has lead to the need for ever more accurate aeroacoustic prediction techniques. One of the most significant noise sources on the high-bypass ratio systems in use (and on the ultra-high bypass contrafan systems currently being planned) is the interaction between wakes shed by an upstream rotating blade row, such as the fan or the rotor rows in the compressor, and a downstream obstacle, such as the outlet guide vanes in the case of the fan or the stators in the case of the compressor. A proper

understanding of the mechanisms involved and an ability to predict the resulting noise are both essential, and these issues are addressed in this paper.

The usual approach, which will be adopted here, is to suppose that the stator row can be unrolled into an infinite two-dimensional cascade of blades, and this is a good approximation provided that strong radial flows are not present. The incident wake distribution, which consists of vorticity and entropy fluctuations, is then taken to be steady in a frame moving with the forward row, so that in the stator frame it can be decomposed into a series of circumferential modes, which for the cascade geometry reduce to harmonic gusts convected by the local mean flow. The first numerical solution to this sort of problem, in which the blades were taken as flat plates perfectly aligned with a uniform mean flow, was developed by Smith (1972) – further details are to be found in Whitehead (1987). Since then, considerable effort has been put into developing numerical procedures which take proper account of the non-uniform flow, and typical approaches have involved either solution of the full time-dependent Euler equations, or solution of the nonlinear steady base flow followed by a linearized calculation of the time-dependent perturbation, and a review has recently been given by Verdon (1993). In particular, Atassi and co-workers have solved numerically the linearized equations derived from Goldstein's (1978) version of rapid distortion theory: Atassi, Subramaniam & Scott (1990) and Scott & Atassi (1990) consider an isolated airfoil, while Fang & Atassi (1993) consider a cascade. However, we believe that very considerable progress can also be made on this problem using a blend of analytical and asymptotic techniques, without the need for extensive numerical calculation. Such an approach has the particular benefit of providing a considerable level of physical insight, as well as being the basis for a comprehensive prediction scheme, and we describe the first stages in this analysis here.

One of the key features of the interaction process is the effect of the stator-blade geometry, namely its camber and thickness distributions and the inclination to the oncoming flow. It will be seen that these features act to modify the local flow so as to both distort the incident disturbance, and to affect the resulting sound generation. We therefore propose to treat these three geometrical features separately, and solve a suite of model problems, the solutions to which will be combined at a later stage. Here we consider the effect of blade inclination, or mean loading, for a flat-plate airfoil and future papers will be concerned with the effects of the blade camber and thickness. Further, we concentrate on the practically important forward radiation; the rearward radiation (required for calculation of the passage of acoustic radiation through the engine) and the unsteady lift distribution on the blades (required for fatigue and performance studies) can also be determined, and will be described in future work. We therefore consider the model problem of a cascade of flat plates of zero thickness inclined at an angle δ to the upstream flow, and suppose that vorticity and entropy gusts of reduced frequency k are incident on the cascade from far upstream. In order to make progress, we will take the entirely realistic limits of $\delta \ll 1$ and $k \gg 1$, and our aim will then be to make consistent asymptotic expansions of the unsteady compressible Euler equations in the preferred limit $k\delta = O(1)$.

Our solution extends two previous lines of investigation. The first concerns the interaction between high-frequency convected gusts and an isolated airfoil inclined at a small angle to an oncoming stream, which has been investigated by Myers & Kerschen (1984, 1995) and Kerschen & Myers (1987). They showed that the flow can be described through a number of asymptotic regions, which are then matched together to yield algebraic expressions for the far-field radiation. The inner region

scales on the gust wavelength and is centred on the airfoil leading edge. In this region noise is generated by the interaction between the incident gust and both the airfoil surface and the local mean-flow gradients. Additional discussion of the physics of these sound generation processes can be found in Myers & Kerschen (1995). In the outer region no sound is generated; the incident gust is convected along the streamlines of the non-uniform mean flow, and distorts before reaching the inner region according to Goldstein's (1978) version of rapid distortion theory, while the sound generated in the inner region is refracted as it propagates back to the far field. In addition, a trailing-edge inner region and a transition region across the blade wake are also present.

The second previous line of investigation concerns the interaction between convected gusts and a cascade of flat-plate airfoils aligned parallel to the oncoming stream (i.e. $\delta = 0$). Koch (1971) and Peake (1993) presented solutions based on the Wiener–Hopf technique, the kernel decomposition being completed in terms of a number of rather complicated infinite-product factors. Peake (1992) and Peake & Kerschen (1995*a*) have derived asymptotic representations for high frequencies, rigorously accounting for the multiple scattering and reflection effects in a way that does not rely on the infinite-product decomposition.

Our aim is therefore to combine these two approaches, but it turns out that the previous asymptotic approximations for the zero-incidence cascade problem are too complicated to allow direct extension to the case $\delta \neq 0$. The first step is therefore to derive a physically based high-frequency expansion for $\delta = 0$, in which the point of generation of each radiation component and its subsequent scattering by other blades is determined explicitly, and an asymptotic formula for the modal coefficients of the upstream radiation, which agrees well with exact results, has indeed been determined in this way. This physically based expansion is also fully consistent with Peake's (1992) result. Once this has been completed, the case $\delta \neq 0$ can be investigated. The non-uniform steady flow through the cascade is found via a Prandtl–Glauert transformation and an exact conformal mapping, and the distortion of the gust as it convects from upstream towards the cascade is then determined. The subsequent interaction of the gust with the blade leading edges occurs in regions of size $O(k^{-1})$ around each leading edge, and is treated in the same way as described by Myers & Kerschen (1995) for the isolated blade. This local interaction produces outgoing sound waves, which are then scattered and reflected by the other blades in the cascade, essentially in the way described by our above high-frequency approximation for $\delta = 0$, before eventually reaching an observer in the far field. By combining all these elements, asymptotic expressions for the upstream radiation can be found, and we derive the first two terms in the expansions of both the amplitude and the phase. A number of consistent simplifications arise naturally from the asymptotic analysis, including the facts that the trailing edges of the cascade have no effect on the forward radiation to this order, and that the non-uniformities in the mean flow have no effect on the rescattering of the field from a given leading edge by other leading edges.

The analysis is presented as follows. The basic formulation of the problem is presented in §2. In §3 we investigate the simple case $\delta = 0$, and validate our high-frequency approximation by comparison with an exact numerical solution. The steady flow through the cascade is described in §4 and Appendices, and in §5 we show how the theory presented in §3 is extended to the case $\delta \neq 0$. Sample results, showing that the mean loading can have a very significant effect, are presented, and further results are also given in Peake & Kerschen (1995*b*).

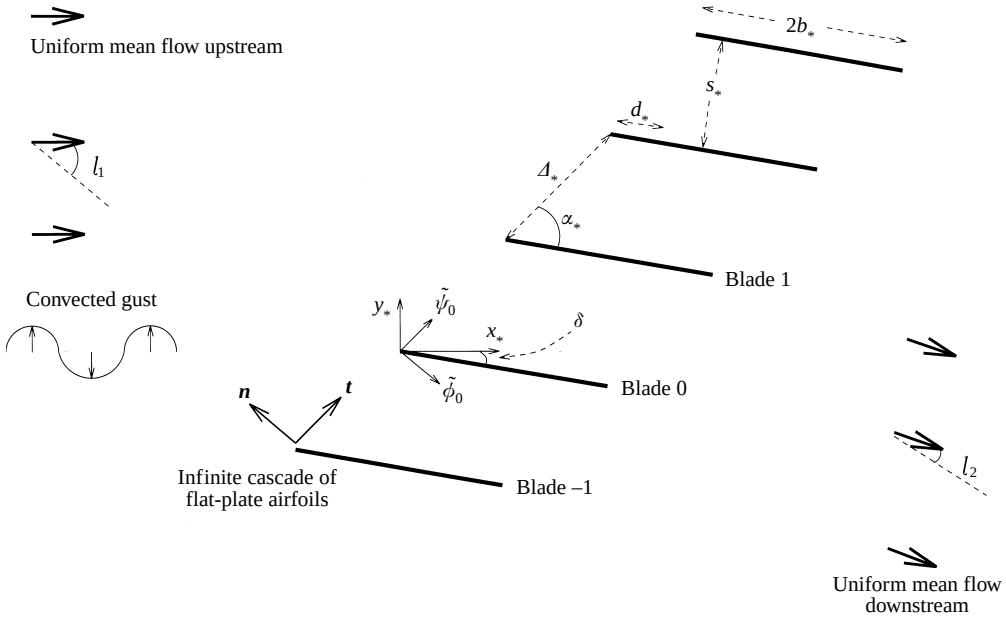

FIGURE 1. The cascade geometry in physical space.

2. Mathematical formulation

We consider an infinite cascade of rigid flat-plate blades, each of chord length $2b_*$, with adjacent leading edges separated by a distance Δ_* and with stagger angle α_*; the corresponding transverse and longitudinal edge separations are s_* and d_*, respectively (we use the suffix $_*$ to denote lengths and angles in physical space). We note that in practice $\Delta_* = O(b_*)$ and $\alpha_* = O(1)$. Far upstream of the cascade there is a uniform steady subsonic mean flow of speed U_∞, which is aligned at an angle δ to the blade chords, and the upstream Mach number is $M_\infty = U_\infty/c_\infty < 1$, with c_∞ the uniform upstream sound speed. The x_*- and y_*-axes are chosen as in figure 1, with the x_*-axis aligned parallel to the upstream flow, and the blades are supposed to have an infinite span in the z_*-direction. The blades are labelled $n = 0, \pm 1, \pm 2, \ldots$, as shown. In the very simple case of $\delta = 0$, the inviscid flow through the cascade is a uniform stream and the blades experience zero mean loading, but when $\delta \neq 0$ the on-coming flow is deflected by the cascade resulting in mean flow gradients and a steady lift force on the blades – we denote the steady flow velocity as $\boldsymbol{U}$. In this paper we aim to investigate the effects of this non-uniform flow on the sound generation properties of the cascade.

We suppose that weak vortical and entropic disturbances, of typical non-dimensional amplitude ϵ with $\epsilon \ll 1$, are present far upstream, which are convected and distorted by the steady non-uniform base flow and interact with the cascade to produce noise. This process is best described using Goldstein's (1978) version of rapid distortion theory, in which the unsteady velocity field, $\boldsymbol{u}'$, is considered as a small perturbation to the steady base flow $\boldsymbol{U}$, and is written in the form

$$\boldsymbol{u}' = \nabla G' + \boldsymbol{v}', \tag{2.1}$$

where $\boldsymbol{v}'$ contains the upstream vorticity fluctuations as well as vorticity generated by interaction with the non-uniform mean flow. The field $\boldsymbol{v}'$ can be determined

analytically, while the unsteady velocity potential G' satisfies an inhomogeneous form of the convected wave equation describing linear disturbances to the non-uniform base flow (equation 2.30 in Goldstein 1978). The vortical field $\boldsymbol{v}'$ appears both in the volume source and in the boundary condition which G' satisfies on the blade surfaces.

We now proceed as in Myers & Kerschen (1995), and transform from the physical coordinates x_* and y_* to non-dimensional steady-flow potential and streamfunction coordinates ϕ and ψ. The dimensional steady velocity field is given in terms of the physical potential and streamfunction by

$$\boldsymbol{U} = \left(\frac{\partial \phi_*}{\partial x_*}, \frac{\partial \phi_*}{\partial y_*}\right) = \left(\frac{\rho_\infty}{\rho_*}\frac{\partial \psi_*}{\partial y_*}, \frac{-\rho_\infty}{\rho_*}\frac{\partial \psi_*}{\partial x_*}\right), \tag{2.2}$$

where ρ_* is the steady local fluid density which takes the value ρ_∞ at upstream infinity, and then ϕ and ψ are given simply by

$$\phi = \phi_*/U_\infty b_*, \quad \psi = \beta_\infty \psi_*/U_\infty b_* \tag{2.3}$$

respectively, with $\beta_\infty = (1 - M_\infty^2)^{1/2}$. This transformation will prove particularly advantageous, since the upstream disturbances are convected along the mean flow streamlines, and the gust distortion will be given in a convenient form. We now suppose that the upstream vortical and entropic disturbances are just harmonic waves with dimensional frequency ω, so that

$$\left.\begin{aligned} \boldsymbol{v}' &\sim \epsilon U_\infty (A_t, A_N, A_z) \exp(\mathrm{i}k[\phi + k_n\psi + k_z z - t]), \\ s' &\sim 2c_p \epsilon B \exp(\mathrm{i}k[\phi + k_n\psi + k_z z - t]), \end{aligned}\right\} \tag{2.4}$$

as $\phi \to -\infty$, where $k = \omega b_*/U_\infty$ is the aerodynamic reduced frequency, $z = z_*/b_*$ is the normalized spanwise coordinate, c_p is the specific heat at constant pressure, and time t has been normalized by b_*/U_∞. By mass conservation it follows that $\boldsymbol{v}'$ is solenoidal upstream, and this in turn leads to the restriction

$$A_t + A_N k_n \beta_\infty + A_z k_z = 0. \tag{2.5}$$

Given the upstream form of the gust, Kerschen & Balsa (1981) have determined $\boldsymbol{v}'$ and s' everywhere in the fluid in the form

$$\left.\begin{aligned} \boldsymbol{v}' &= \epsilon U_\infty \left(\frac{A_t^* U_\infty}{|\boldsymbol{U}|} + \frac{B|\boldsymbol{U}|}{U_\infty}, \rho_* \frac{|\boldsymbol{U}|}{\rho_\infty U_\infty}\left[A_N + \beta_\infty A_t^* \frac{\partial g}{\partial \psi}\right], A_z\right) \exp(\mathrm{i}k\chi), \\ s' &= 2c_p \epsilon B \exp(\mathrm{i}k\chi), \end{aligned}\right\} \tag{2.6}$$

where

$$\chi = \phi + k_n\psi + k_z z + g(\phi, \psi) - t, \tag{2.7}$$

the quantity A_t^* is

$$A_t^* = A_t - B \tag{2.8}$$

and $g(\phi, \psi)$ is Lighthill's drift function

$$g(\phi, \psi) = \int_{-\infty}^{\phi} \left[\frac{U_\infty^2}{|\boldsymbol{U}|^2(\xi, \psi)} - 1\right] \mathrm{d}\xi. \tag{2.9}$$

The drift function represents the cumulative distortion of vortex lines approaching the cascade; far upstream, in the limit $\phi \to -\infty$, we see that $g \to 0$ and that (2.4) is regained from (2.6). The quantity A_t^* expresses the fact that the interaction between the entropy fluctuation and the non-uniform mean flow generates additional velocity

fluctuations, while the entropy fluctuation itself is simply convected with the mean flow.

We now suppose that the incidence angle δ satisfies $\delta \ll 1$, so that the steady flow takes the form of uniform flow U_∞ plus a small non-uniform perturbation of size $O(\delta)$, and this perturbation can then be described in terms of the complex potential $\delta F(\zeta)$, where $\zeta = \phi + \mathrm{i}\psi$. In §4 a Prandtl–Glauert transformation will be used to relate $\delta F(\zeta)$ to the complex potential for an incompressible flow through a cascade, which can in turn be determined using the theory of conformal mappings. We note here, however, that it is easy to show that $F'(\zeta) = q - \mathrm{i}\mu$, where $\delta U_\infty q$ is the dimensional perturbation to the mean-flow speed U_∞ and $\delta\beta_\infty\mu$ is the perturbation in steady flow angle.

The modified unsteady velocity potential $h(\phi, \psi)$, which is related to the dimensional unsteady velocity potential G' by

$$G' = \epsilon U_\infty b_* h(\phi, \psi) \exp(\mathrm{i}k[k_z z - t - M_\infty^2 \phi/\beta_\infty^2]) \exp(\delta M_\infty^2 q), \tag{2.10}$$

is now introduced, and we suppose further that $\epsilon \ll \delta \ll 1$, so that the unsteady disturbances are much smaller than the steady disturbance produced by the mean loading. (This assumption is often valid for blade-row interactions of interest in applications and will make the subsequent analysis tractable, in particular allowing the gust to be treated as a small perturbation to the non-uniform steady flow.) In this limit, Kerschen & Myers (1986) were able to show that Goldstein's equation for G' reduces to

$$(\mathscr{L}_0 + \delta\mathscr{L}_1)(h) = \delta k S(\phi, \psi) \exp(\mathrm{i}k\Omega), \tag{2.11}$$

where the operator $\mathscr{L}_0$ is simply the Helmholtz operator with wavenumber kw, and w is defined by

$$w^2 = (M_\infty/\beta_\infty^2)^2 - (k_z/\beta_\infty)^2. \tag{2.12}$$

The quantity kw is the acoustic reduced frequency. The source term on the right-hand side of (2.11) indicates the presence of volume sound sources in the flow, which arise due to the interaction of the convected disturbances and the mean flow gradients. Myers & Kerschen (1995) showed that, in the high-frequency limit, the only volume sources which produce significant sound radiation are those located in the neighbourhood of each blade leading edge. The operator $\mathscr{L}_1$ is a second-order operator with variable coefficients which depend on the mean flow, and accounts for the refraction of sound waves propagating through the non-uniform steady flow. The complicated expressions for $\mathscr{L}_1$ and $S\exp(\mathrm{i}k\Omega)$ are given by Myers & Kerschen (1995, equations 2.5*a*,*b*), and need not be repeated here.

The zero-normal-velocity boundary condition on the blade surfaces can be transformed into ϕ, ψ space in a straightforward manner, and it turns out that

$$\frac{\partial h}{\partial \psi} + \delta M_\infty^2 \frac{\partial q}{\partial \psi} h = -\left[\frac{A_N}{\beta_\infty}(1 - \delta M_\infty^2 q) - 2\delta A_t^* \mu\right] \exp(\mathrm{i}k\Omega) \tag{2.13}$$

applied on the blade surfaces, where the left-hand side corresponds to the cross-stream velocity component of the irrotational unsteady flow. Again, significant sound radiation is produced only by the contributions from the vicinity of each leading edge. It is also helpful to note here that the dimensional acoustic pressure, p', is given by

$$p' = -\epsilon\rho_\infty U_\infty^2 \left\{\left[\frac{\partial h}{\partial \phi} - \mathrm{i}\frac{k}{\beta_\infty^2} h\right] \exp(\mathrm{i}k[k_z z - t - M_\infty^2 \phi/\beta_\infty^2])\right\}. \tag{2.14}$$

Finally, given the spatial periodicity of the steady flow and of the incident gusts,

it follows that when considered as a function of position $\boldsymbol{x}_*$ in physical space, the unsteady velocity potential G' obeys the quasi-periodic condition

$$G'(\boldsymbol{x}_* + \Delta_* \boldsymbol{t}, t) = \exp(\mathrm{i}\sigma) G'(\boldsymbol{x}_*, t), \tag{2.15}$$

where $\boldsymbol{t}$ is the unit vector along the front face of the cascade (see figure 1) and σ is the gust inter-blade phase angle

$$\sigma = kd + kk_n s, \tag{2.16}$$

where s and d are the transverse and longitudinal separations of the blades in ϕ, ψ space (see figure 5). The modified potential $h(\phi, \psi)$ satisfies the corresponding quasi-periodicity condition

$$h(\phi + d, \psi + s) = \exp(\mathrm{i}\sigma') h(\phi, \psi), \tag{2.17}$$

where the modified inter-blade phase angle σ' is given by

$$\sigma' = \sigma + \frac{kM_\infty^2 d}{\beta_\infty^2}. \tag{2.18}$$

It is easy to see that when $\delta = 0$ the boundary-value problem specified by (2.11)–(2.15) reduces to the usual unloaded cascade problem studied by Koch (1971) and Peake (1993). Our aim here is to determine the first two terms in the amplitude and the phase of the asymptotic solution of (2.11)–(2.15) with $\delta \ll 1$, $k \gg 1$ and $k\delta = O(1)$, and hence to derive the correction to the forward radiation for non-zero δ. Specifically, it turns out that the modified unsteady velocity potential ahead of the cascade is composed of a superposition of plane-wave modes, each of the form

$$(a_0 + a_1 + \ldots) \exp(\mathrm{i}b_0 + \mathrm{i}b_1 + \ldots), \tag{2.19}$$

where $a_0 = O(k^{-2})$, $a_1 = O(k^{-5/2}, \delta k^{-3/2})$, $b_0 = O(k)$ and $b_1 = O(k\delta)$. In this paper we determine $a_{0,1}$ and $b_{0,1}$. Before doing this, however, we need to reconsider the cascade problem for $\delta = 0$, in order to cast its solution into a form suitable for the extension envisaged above, and this will be described in the next section.

3. Unsteady flow for zero mean loading

The scattering of upstream disturbances by a cascade of flat plates aligned parallel to a uniform mean flow, and related problems, have been investigated by a number of authors (see the references in Peake 1992), and the solution is completed using the Wiener–Hopf technique to yield expressions for the radiation in terms of a number of infinite-product factors. The difficulty with these results, however, is that the various terms cannot be given a straightforward physical interpretation, and so cannot be extended to include the effects of mean loading. In this section we therefore derive an alternative and more physically based description of the case of zero mean loading ($\delta = 0$), based on our high-frequency limit $k \gg 1$. Once this has been done the extension to the case $\delta \neq 0$ will be completed in §§4 and 5. Here, we calculate the first two terms in the high-frequency expansion of the radiation ahead of the cascade, thereby extending the earlier work of Envia & Kerschen (1986), who found just the first term.

We note first that the steady-flow potential and streamfunction for zero mean loading, denoted ϕ_0 and ψ_0 respectively, are simply proportional to the physical coordinates, and that the cascade in physical space maps onto a cascade in ϕ_0, ψ_0 space (or Prandtl–Glauert space) with chord length 2, with stagger angle $\alpha_0 = \tan^{-1} \beta_\infty s_*/d_*$

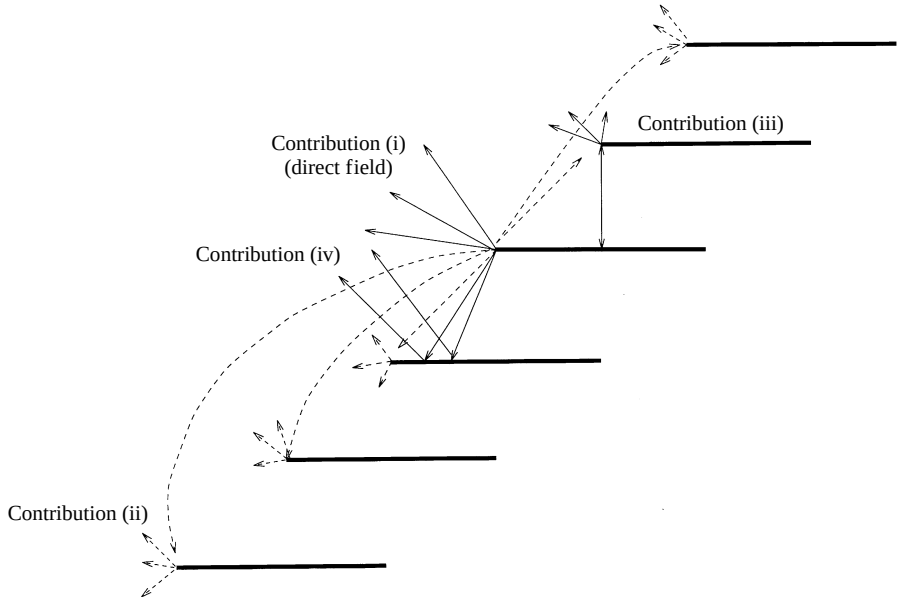

FIGURE 2. The principal radiation components reaching an upstream observer for $kw \gg 1$.

and with a separation between adjacent leading edges of

$$\Delta_0 = (d_*^2 + \beta_\infty^2 s_*^2)^{1/2}/b_*. \tag{3.1}$$

We fix the arbitrary constants associated with the potential and streamfunction by supposing that the leading edge of the zeroth blade is mapped onto the origin in ϕ_0, ψ_0 space. Here, and in what follows, the suffix $_0$ indicates that we are considering the case $\delta = 0$. We note here that when $\delta = 0$ the normal velocity boundary condition (2.13) reduces to $\partial h/\partial \psi_0 = -(A_N/\beta_\infty)\exp(\mathrm{i}k\phi/\beta_\infty^2)$.

The high-frequency parameter for the cascade analysis of this section is the wavenumber kw appearing in the Helmholtz operator $\mathscr{L}_0$, which is an effective acoustic reduced frequency for the field $h(\phi, \psi)$ based on the airfoil semi-chord b_* and the projected acoustic wavelength in the two-dimensional ϕ, ψ space. The effects of the mean flow and of disturbance three-dimensionality on the projected acoustic wavelength are contained in the parameter w. In our analysis for the general case $\delta \neq 0$ we must consider the evolution of both convected and acoustic disturbances, and we shall therefore take the formal limit $k \gg 1$, $w = O(1)$. For the high subsonic Mach numbers of practical interest, however, we see that typically $w > 1$, suggesting that our asymptotic approximations will be valid for a wider range of k than might at first have been supposed, and this will be confirmed in §3.4. When w is small, for instance for a highly swept gust for which k_z is near M_∞/β_∞, the high-frequency approach described here cannot be applied for realistic values of k, but such cases seem of less practical interest and will be ignored.

3.1. *Identification of the radiation components*

In the limit $kw \gg 1$, it can be shown that the radiation reaching an observer in the far field ahead of the cascade consists of the four components illustrated in figure 2. These components arise as follows:

(i) sound is generated by the interaction between the gust and each blade leading edge, and propagates directly to the observer without interacting with any other blades

– this is exactly equivalent to the radiation produced by the interaction between the gust and an isolated leading edge, and is referred to as the *direct field*, as calculated by Envia & Kerschen (1986);

(ii) the direct field from a given leading edge will travel along the front face of the cascade according to a complicated Fresnel-diffraction process, and will interact with all the other leading edges to produce more radiation, some of which will then travel directly to the observer;

(iii) from a given leading edge, the direct field in the negative ψ_0-direction will be reflected by the lower blade and then rescattered by the leading edge from which it originated. Some of this rescattered field will then reach the observer directly and some will be rereflected by the lower blade back to the leading edge, and the process will continue indefinitely;

(iv) for a staggered cascade the total field emitted from a given leading edge in the sector $\pi + \alpha_0 < \theta < 3\pi/2$ is reflected by the adjacent lower blade, before reaching the observer.

The total unsteady field ahead of the cascade is of course composed of many more components, including the multiple rescattering by other leading edges, and the radiation produced by the complicated interactions between these components and the trailing edges of the cascade. However, since the modified velocity potential of the direct field is $O((kw)^{-3/2})$ and since the leading-edge diffraction coefficient is proportional to $(kw)^{-1/2}$, it is clear that contributions to the radiation which emanate from one given leading edge and are then rescattered more than once before reaching the observer will be $O((kw)^{-5/2})$ or smaller, and will not feature in the first two terms in our asymptotic expansion. In addition, the effects of the trailing edges do not arise to this asymptotic order, but we will delay full justification of this point until after the first two terms have been calculated; we merely note at this stage that since the trailing edge can be neglected, the blades are taken to be semi-infinite in the positive ϕ_0-direction when calculating the four contributions described above.

By using Fourier transforms and the Wiener–Hopf technique and then applying the method of steepest descents (the analysis is described in detail in the context of acoustic wave scattering in chapter 2 of Noble 1988; the gust interaction prolem, including extensions to account for mean-loading effects, is described in Myers & Kerschen 1995), it is straightforward to show that the far-field limit of the modified unsteady velocity potential, $h(\phi_0, \psi_0)$, for the direct field generated by the incident gust striking the leading edge of blade n is

$$\frac{A_N D_0(\theta_n, -1/\beta_\infty^2) \exp(\mathrm{i}kwr_n + \mathrm{i}n\sigma_0')}{k^{3/2}\beta_\infty r_n^{1/2}}, \tag{3.2}$$

where the distance r_n and angle θ_n ($0 < \theta_n < 2\pi$) are the observer polar coordinates in ϕ_0, ψ_0 space relative to the leading edge of the nth blade, and the directivity D_0 is given by

$$D_0(\theta, \mu) = \frac{\exp(-\mathrm{i}\pi/4)\cos\theta/2}{\pi^{1/2}(w\cos\theta + \mu)(w - \mu)^{1/2}}. \tag{3.3}$$

The factor $\cos\theta/2$ is characteristic of edge radiation. In addition, the modified inter-blade phase angle σ_0' can be found by replacing s and d in (2.16) and (2.18) by s_0 and d_0. It should be noted that the field decays cylindrically away from the leading edge, and corresponds to the radiation from an effective point source (of fractional order $\frac{3}{2}$) located at the leading edge of blade n. This is contribution (i).

We now consider contribution (ii). The direct field from, say, blade 0 will travel along the front face of the cascade and will be scattered by all the other blade leading edges, and in order to calculate the radiation produced we need to know the fraction of this direct field reaching the leading edge of blade n, for each n. The case $n = \pm 1$ is trivial, and the case $n = \pm 2$ can be completed using Macdonald's formula (in Goldstein 1976) for the radiation generated by a point source separated from the observer by a rigid half-plane. However, it does not seem possible to generalize Macdonald's result to the case of more than one intervening half-plane, particularly in view of the fact that we need to know the field along a geometrical optics boundary, which must necessarily be governed by a complicated Fresnel-diffraction process. However, Lee (1978) has shown, in the electromagnetic context that to leading order in (large) k the proportion of the direct field from blade 0 reaching the leading edge of blade n is simply the direct field which would have arrived if no intervening blades had been present, multiplied by the factor $1/n$; when $n = 2$, this simple result reduces to the high-frequency limit of Macdonald's formula. In physical terms, the Fresnel component of the radiation is retained (for which the unsteady velocity potential is $O((kw)^{-3/2})$, while the diffracted components generated by the scattering of the direct field at each intervening blade leading edge are $O((kw)^{-2})$ and are neglected by Lee. It follows that the accuracy of Lee's result is entirely consistent with the order of our asymptotic expansion. The direct field from the leading edge of blade 0 therefore decays like $n^{-3/2}$ along the front face of the cascade, thanks to a combination of Lee's result and cylindrical spreading. (It is worth noting that the application of Lee's result to the present problem has been facilitated by the transformation (2.10), which leads to the appearance of the Helmholtz operator at leading order in (2.11)). It turns out that contribution (iii) can be treated in exactly the same way as (ii), because the component of the re-radiated sound in the back-scattered direction is governed by the same Fresnel process as the field propagating along the front face; the fraction of the direct field which returns to the leading edge after n reflections by the lower blade is simply $1/n$ to leading order in k.

Since $kw \gg 1$ and $\Delta_* = O(b_*)$, each leading edge is in the acoustic far field of a source located at any other leading edge, so that the far-field form of the direct field, as given in (3.3), can be used in calculating the above components. It therefore follows that the total sound field which falls on the leading edge of blade n can be calculated using these results, and is found to have unsteady velocity potential

$$\frac{\exp(\mathrm{i}n\sigma_0')}{k^{3/2}}\left[B_0^1\exp(-\mathrm{i}kw(\cos\alpha_0\phi_0^n+\sin\alpha_0\psi_0^n))+B_0^2\exp(\mathrm{i}kw(\cos\alpha_0\phi_0^n+\sin\alpha_0\psi_0^n))\right.$$
$$\left.+B_0^3\exp(\mathrm{i}kw\psi_0^n)\right]+O\left((kw)^{-2}\right), \qquad (3.4)$$

where

$$\left.\begin{aligned} B_0^1 &= \sum_{m=1}^{\infty}\left\{\frac{A_N D_0(\pi+\alpha_0,-1/\beta_\infty^2)\exp(\mathrm{i}kwm\Delta_0+\mathrm{i}m\sigma_0')}{\beta_\infty m^{3/2}\Delta_0^{1/2}}\right\},\\ B_0^2 &= \sum_{m=1}^{\infty}\left\{\frac{A_N D_0(\alpha_0,-1/\beta_\infty^2)\exp(\mathrm{i}kwm\Delta_0-\mathrm{i}m\sigma_0')}{\beta_\infty m^{3/2}\Delta_0^{1/2}}\right\},\\ B_0^3 &= \sum_{m=1}^{\infty}\left\{\frac{A_N D_0(3\pi/2,-1/\beta_\infty^2)\exp(2\mathrm{i}kwms_0)}{\beta_\infty m^{3/2}(2s_0)^{1/2}}\right\}. \end{aligned}\right\} \qquad (3.5)$$

In (3.4), the alternative coordinates ϕ_0^n, ψ_0^n are centred on the nth leading edge, the first term corresponds to the direct fields from the leading edges of blades $n+1, n+2, \ldots$, the second term to the direct fields from blades $n-1, n-2, \ldots$ and the third term is the multiply reflected contribution referred to in (iii) above. Now that we have calculated the acoustic radiation falling on the nth leading edge, it is an easy matter to find the radiation reaching the far field: the total radiation (excluding contribution (iv) for the moment) reaching an upstream observer from leading edge n is simply the sum of the direct field (3.2) and the field generated by the scattering of the incident field (3.4). We write the unsteady velocity potential for this radiation as $f_0^n(\phi_0^n, \psi_0^n)$, and using the same approach as was used in calculating the direct field (3.2) find that upstream

$$f_0^n(\phi_0^n, \psi_0^n) = \frac{\exp(\mathrm{i}kwr_n + \mathrm{i}n\sigma_0')}{k^{3/2} r_n^{1/2}} \left\{ \frac{A_N}{\beta_\infty} D_0(\theta_n, -1/\beta_\infty^2) - \frac{\mathrm{i}B_0^1 w \sin\alpha_0}{k^{1/2}} D_0(\theta_n, w\cos\alpha_0) + \frac{\mathrm{i}wB_0^2 \sin\alpha_0}{k^{1/2}} D_0(\theta_n, -w\cos\alpha_0) + \frac{\mathrm{i}wB_0^3}{k^{1/2}} D_0(\theta_n, 0) \right\}. \quad (3.6)$$

Finally, we now take account of contribution (iv) by noting that the reflection of the field (3.6) by the adjacent lower blade can be represented by introducing an image source at the point $(\phi_0^n = 0, \psi_0^n = -2s_0)$, and that the observer in the far field will only receive a contribution from this image provided that $\pi/2 < \theta_n < \pi - \alpha_0$. We have therefore calculated the far-field radiation emanating from the leading edge of blade n, and the unsteady velocity potential of the total radiation reaching the observer in the far field is then simply obtained by adding together the radiation from each leading edge, and has unsteady potential

$$h_0(\phi_0, \psi_0) = \sum_{n=-\infty}^{\infty} \Big[f_0^n(\phi_0^n, \psi_0^n) + f_0^n(\phi_0^n, -\psi_0^n - 2s_0) \{ \mathrm{H}(\theta_n - \pi/2) - \mathrm{H}(\theta_n - \pi + \alpha_0) \} + O((kw)^{-5/2}) \Big], \quad (3.7)$$

where H is the unit step function, and the second term in the summation arises from the reflection by the lower blade.

3.2. *Determination of the modal structure*

The above analysis has made it clear that, at high frequency, the radiation ahead of the cascade can be thought of as being generated by a point source located at each blade leading edge. The field of each point source decays cylindrically with distance, but when these individual components are added together we will find that the total radiation is in fact composed of plane-wave modes ahead of the cascade. This is best seen by employing the technique described by Envia & Kerschen (1986), and since their analysis was for an unstaggered cascade we will describe here the main steps in the more general approach for non-zero stagger. We begin by defining new coordinates $\tilde{\phi}_0$ and $\tilde{\psi}_0$ centred on the leading edge of blade 0 but aligned perpendicular to and along the front face of the cascade, respectively, and with the $\tilde{\phi}_0$-axis pointing downstream. We then note that the phase difference between the unsteady fields from adjacent leading edges is simply σ_0', and write

$$f_0^n(\phi_0^n, \psi_0^n) \equiv \frac{F(\theta_n)}{r_n^{1/2}} \exp(\mathrm{i}n\sigma_0' + \mathrm{i}kwr_n), \quad (3.8)$$

where expressions for r_n and θ_n in terms of $\tilde{\phi}_0$ and $\tilde{\psi}_0$ can easily be derived, and where $F(\theta_n)$ is independent of n except through its argument θ_n. For clarity, we consider just

the first series in (3.7) – i.e. the field without the reflection – and include the second term later. We proceed by expressing each term in this series as an integral over a new coordinate ξ in the $\tilde{\psi}_0$-direction by use of the Dirac delta function to give

$$\sum_{n=-\infty}^{\infty} f_0^n(\phi_0^n, \psi_0^n) = \sum_{n=-\infty}^{\infty} \int_{-\infty}^{\infty} \frac{F(\theta_n(\xi))}{(\tilde{\phi}_0^2 + \xi^2)^{1/4}} \exp(\mathrm{i}n\sigma_0' + \mathrm{i}kw(\tilde{\phi}_0^2 + \xi^2)^{1/2})\delta(\xi - \tilde{\psi}_0 + \Delta_0 n)\mathrm{d}\xi. \tag{3.9}$$

By exchanging the orders of integration and summation, re-expressing the resulting sum of delta functions as a sum of exponentials using Poisson's summation formula (see Jones 1966, p. 137) in the form

$$\sum_{n=-\infty}^{\infty} \exp(\mathrm{i}n\sigma_0')\delta(\Delta_0 n + \xi - \tilde{\psi}_0) = \frac{1}{\Delta_0} \sum_{n=-\infty}^{\infty} \exp(\mathrm{i}(\xi - \tilde{\psi}_0)(2\pi n - \sigma_0')/\Delta_0), \tag{3.10}$$

and applying the transformation $\xi = |\tilde{\phi}_0|\zeta$, we find that

$$\sum_{n=-\infty}^{\infty} f_0^n(\phi_0^n, \psi_0^n) = \frac{|\tilde{\phi}_0|^{1/2}}{\Delta_0} \sum_{n=-\infty}^{\infty} \exp(-\mathrm{i}\tilde{\psi}_0(2n\pi - \sigma_0')/\Delta_0) \int_{-\infty}^{\infty} \frac{F(\theta_n(\zeta))}{(1+\zeta^2)^{1/4}} \exp(|\tilde{\phi}_0|\mathscr{F}(\zeta))\mathrm{d}\zeta. \tag{3.11}$$

Here we have

$$\mathscr{F}(\zeta) = \mathrm{i}kw(1+\zeta^2)^{1/2} + \mathrm{i}(2n\pi - \sigma_0')\zeta/\Delta_0, \tag{3.12}$$

and $\theta_n(\zeta)$ has now become independent of n thanks to the replacement of $\tilde{\psi}_0$ by ξ (or ζ), and is given by

$$\theta_n(\zeta) \equiv \theta(\zeta) = \tan^{-1}\left[\frac{\zeta \sin\alpha_0 - \mathrm{sgn}(\tilde{\phi}_0)\cos\alpha_0}{\zeta\cos\alpha_0 + \mathrm{sgn}(\tilde{\phi}_0)\sin\alpha_0}\right]. \tag{3.13}$$

Since our aim is to determine the far-field radiation upstream, we now apply the limit $\tilde{\phi}_0 \to -\infty$ and use the method of steepest descents to evaluate the limiting form of (3.11). It turns out that for each n, $\mathscr{F}(\zeta)$ possesses a single saddle point at

$$\zeta_{0s}^n = \frac{-(2n\pi - \sigma_0')}{[\Delta_0^2 k^2 w^2 - (2n\pi - \sigma_0')^2]^{1/2}}, \tag{3.14}$$

so that the integral in (3.11) is dominated by contributions from the neighbourhood of $\zeta = \zeta_{0s}^n$. There is a finite range of n for which ζ_{0s}^n is real; these correspond to propagating plane-wave modes. For other values of n the saddle point ζ_{0s}^n is imaginary; these correspond to modes that are exponentially attenuated with upstream distance and can be neglected in calculating the far-field radiation. After some considerable, but straightforward manipulation we find that

$$\sum_{n=-\infty}^{\infty} f_0^n(\phi_0^n, \psi_0^n) \sim \sum_{n=-r_0}^{q_0} \mathscr{R}_n(\theta(\zeta_{0s}^n)) \exp(-\mathrm{i}\sigma_0^n\phi_0 - \mathrm{i}\eta_0^n\psi_0) \quad \text{as} \quad \tilde{\phi}_0 \to -\infty, \tag{3.15}$$

where the coefficients $\mathscr{R}_n(\theta)$ are given by

$$\begin{aligned}\mathscr{R}_n(\theta) = \frac{\exp(\mathrm{i}\pi/4)(2\pi)^{1/2}w^{1/2}}{k\left[\Delta_0^2k^2w^2 - (2n\pi - \sigma_0')^2\right]^{1/2}} \Bigg[&\frac{A_N}{\beta_\infty} D_0\left(\theta, -1/\beta_\infty^2\right) \\ &- \frac{\mathrm{i}B_0^1 w\sin\alpha_0}{k^{1/2}} D_0(\theta, w\cos\alpha_0) + \frac{\mathrm{i}B_0^2 w\sin\alpha_0}{k^{1/2}} D_0(\theta, -w\cos\alpha_0) \\ &+ \frac{\mathrm{i}B_0^3 w}{k^{1/2}} D_0(\theta, 0)\Bigg] + O((kw)^{-3})\end{aligned} \tag{3.16}$$

and the modal wavenumbers σ_0^n and η_0^n are

$$\left.\begin{aligned}\sigma_0^n &= [(2n\pi - \sigma_0')\cos\alpha_0 + \sin\alpha_0(\Delta_0^2 k^2 w^2 - (2n\pi - \sigma_0')^2)^{1/2}]/\Delta_0,\\ \eta_0^n &= [(2n\pi - \sigma_0')\sin\alpha_0 - \cos\alpha_0(\Delta_0^2 k^2 w^2 - (2n\pi - \sigma_0')^2)^{1/2}]/\Delta_0,\end{aligned}\right\} \tag{3.17}$$

where n is now the mode index. The cut-on modes satisfy $-r_0 \leqslant n \leqslant q_0$, where $-r_0$ and q_0 are the smallest and largest values of n for which the square-root in (3.17) is real. At this point we return to (3.7), include the second series in exactly the same way as above and transform back to physical coordinates, to find that the far-field limit of the modified unsteady velocity potential ahead of the cascade is given as a superposition of radiating plane-wave modes in the form

$$\sum_{n=-r_0}^{q_0} R_n(\theta(\zeta_{0s}^n))\exp(-\mathrm{i}\sigma_0^n x_*/b_* - \mathrm{i}\eta_0^n \beta_\infty y_*/b_*), \tag{3.18}$$

where

$$\begin{aligned}R_n(\theta) &= \mathscr{R}_n(\theta) + \mathscr{R}_n(2\pi - \theta)\exp(-2\mathrm{i}s_0\eta_0^n)\{\mathrm{H}(\theta - \pi/2) - \mathrm{H}(\theta - \pi + \alpha_0)\}\\ &= \mathscr{R}_n(\theta)\left[1 - \exp(-2\mathrm{i}s_0\eta_0^n)\{\mathrm{H}(\theta - \pi/2) - \mathrm{H}(\theta - \pi + \alpha_0)\}\right],\end{aligned} \tag{3.19}$$

and the second step in (3.19) has been completed by noting that $D_0(\theta) = -D_0(2\pi - \theta)$.

To summarize, we have found the modal representation of the modified potential of the acoustic field upstream of the cascade, in the large-kw limit. The first two terms of the asymptotic expansion in kw have been derived. For large kw, the number of propagating modes is proportional to kw; the first two terms in the asymptotic expansions for the modal coefficients R_n are seen from (3.16) to be of $O((kw)^{-2})$ and $O((kw)^{-5/2})$ respectively. Note also that equation (3.18) is consistent with Peake's (1992) results, in that if an expression for the upstream radiation is derived using his method and then expanded for high reduced frequency, then the resulting first two terms agree exactly with (3.18). It is again emphasized, however, that the present method, in which the generation and propagation of each radiation component is derived explicitly, is the only analytical approach which allows the extension to non-uniform mean flow.

3.3. *Neglect of trailing edges*

We recall that our asymptotic expansion has been derived by assuming that the trailing edges of the cascade can be neglected, and we are now in a position to justify this. It is clear from (3.16) that the direct field (contribution i) produces modes ahead of the cascade with amplitude $O((kw)^{-2})$, i.e. the first term in (3.16), and it could also be shown (see Peake 1992, p. 271, equation 28) that downstream-travelling duct modes of amplitude $O((kw)^{-2})$ which propagate in the passages between adjacent blades are also generated. These duct modes interact with the trailing edges of the cascade to generate both downstream radiation and reflected duct modes travelling back upstream. The reflected duct modes have size $O((kw)^{-3})$ (see Peake 1992, p. 276, equations 45 and 46), and will interact with the leading edges of the cascade to generate more upstream radiation, in excess of that already calculated in (3.16), and thereby provide a correction to our expression for the R_n. However, this radiation correction will be no larger than the upstream-travelling duct modes which generated it, i.e. $O((kw)^{-3})$, and since our aim is only to calculate the first two terms in the forward radiation, which are size $O((kw)^{-2})$ and $O((kw)^{-5/2})$ respectively, it is clear that this trailing-edge correction is smaller than the second term in (3.16) by a factor $O((kw)^{-1/2})$, and is therefore ignored.

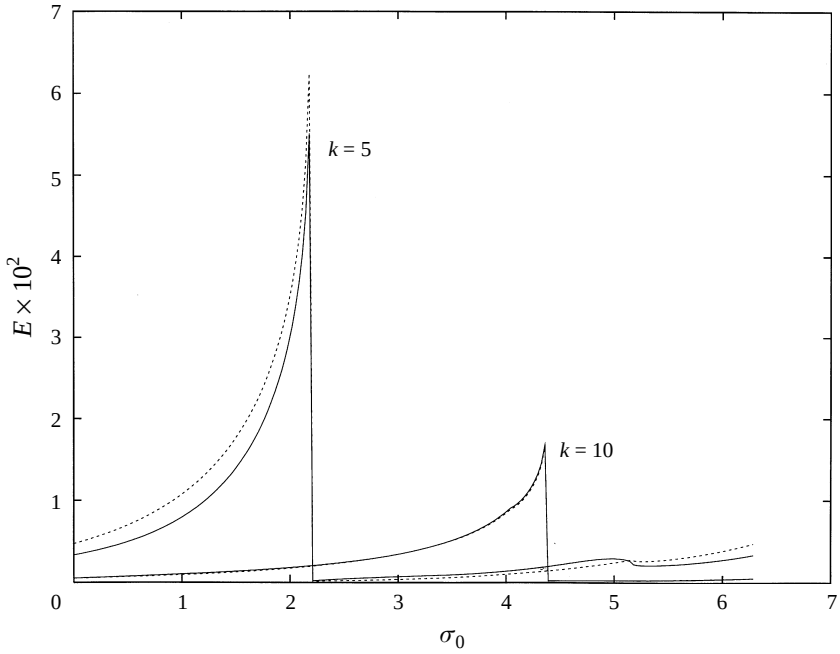

FIGURE 3. Plots of the normalized acoustic energy flux ahead of the cascade, E, for varying values of the inter-blade phase angle σ_0 with $M_\infty = 0.8$, $s_*/b_* = 2$, $d_*/b_* = 1$, $A_N = 1$ and for $k = 10$ and $k = 5$. The solid lines are the results from the exact solution, and the dashed lines from the approximate solution in which the trailing edges are neglected.

In addition to this asymptotic argument, the relatively small effect exerted by the trailing edges on the forward-radiated noise for high kw can also be confirmed numerically. An exact prescription for determining the radiation generated ahead of a cascade of finite-chord flat-plate blades at zero incidence has been given by Peake (1993), using a pair of coupled Wiener–Hopf problems to determine the duct modes between adjacent blades and hence the radiation-mode amplitudes. Alternatively, the radiation ahead of a cascade in which the trailing edges are completely neglected (so that the chord is taken as semi-infinite) has been predicted by a number of authors using a rather more elementary application of the Wiener–Hopf technique (details in Peake & Kerschen 1995*a*). We compare the predictions of these two theories by examining the normalized acoustic energy flux E radiated upstream of the cascade. The quantity

$$E = \sum_{n=-r_0}^{q_0} (\Lambda_0^2 k^2 w^2 - (2n\pi - \sigma_0')^2)^{1/2} |R_n|^2 \tag{3.20}$$

is proportional to the time-averaged acoustic energy flux per blade, propagating upstream across a surface parallel to the front face of the cascade. In figure 3, the upstream acoustic energy flux E predicted by the exact and the semi-infinite chord theory is plotted as a function of inter-blade phase angle σ_0, for the two cases $k = 5$ and $k = 10$, with $M_\infty = 0.8$ so that $kw = 6.67$ and $kw = 13.33$ respectively. Very good agreement between the exact and approximate results is obtained, confirming that the trailing edges can indeed be neglected when kw is large, with only a small error. The sharp drop in E observed on all the plots corresponds to an upstream radiation mode becoming cutoff.

3.4. *Results and discussion*

Before presenting some results calculated using the above analysis, we first note that our asymptotic expression for R_n becomes infinite at certain isolated critical conditions. From (3.14) it is clear that this happens when the saddle point ζ_{0s}^n approaches infinity, which is when $\sigma_0^n = \pm kw\cos\alpha_0, \eta_0^n = \pm kw\sin\alpha_0$, or equivalently when the mode angle is $\theta(\zeta_{0s}^n) = \pi + \alpha_0, \alpha_0$ respectively. These are exactly the cut-off conditions for upstream-propagating modes, whose propagation direction must lie in the region $\alpha_0 < \theta < \pi + \alpha_0$.

The three directivity functions $D_0(\theta_n, \pm w\cos\alpha_0)$ and $D_0(\theta_n, 0)$ in (3.16) may also become singular. This happens when an upstream-propagating mode approaches cut-off as above, or when the propagation direction of an upstream-propagating mode approaches a shadow boundary associated with the field reflected off the blade below (contributions iii and iv). The propagation direction for the reflected field must lie in the range $\pi/2 < \theta < \pi - \alpha_0$, the two limits forming the shadow boundaries for this field. Specifically, it can be seen from (3.3) that $D_0(\theta_n, w\cos\alpha_0)$ is singular when the mode angle $\theta(\zeta_{0s}^n)$ is equal to either $\pi - \alpha_0$ or $\pi + \alpha_0$; the first of these corresponds to a shadow boundary of the reflected field while the second corresponds to a cut-off condition. The function $D_0(\theta_n, -w\cos\alpha_0)$ is singular when $\theta(\zeta_{0s}^n) = \alpha_0$ corresponding to the other cut-off condition (the angle $\theta = 2\pi - \alpha_0$ is not of interest since it lies outside the region for upstream propagation), and $D_0(\theta_n, 0)$ is singular when $\theta(\zeta_{0s}^n) = \pi/2$ corresponding to the other shadow boundary for the reflected field ($\theta = 3\pi/2$ is also not of interest since it lies outside the region for upstream propagation). In addition, the non-uniformities due to the appearance of the two step-function discontinuities in (3.19) are also related to the the shadow boundaries for the reflected field. We emphasize, however, that these non-uniformities arise only in isolated conditions for which the direction of propagation of an upstream propagating mode approaches a cut-off angle α_0 or $\pi + \alpha_0$, or a shadow boundary angle $\pi/2$ or $\pi - \alpha_0$.

In a previous paper (Peake & Kerschen 1995*a*) we have derived a uniform asymptotic factorization of the generic Wiener–Hopf kernel for the cascade, which remains valid in the vicinity of all these critical ray directions. However, some additional simplification of this latter analysis will be necessary in order to allow its extension to non-zero mean loading, and in this paper we will concentrate on the case in which the modes are both well cut-on and not too close to either of the critical directions $\pi/2$ and $\pi - \alpha_0$, thus avoiding the non-uniformities described above. The regime covered in this paper therefore includes a very considerable portion of all possible parameter values, and so is of considerable practical interest. Note that the interpretation of the critical ray directions given in the final paragraph on p. 183 of Peake & Kerschen (1995*a*) is incorrect.

In figure 4 we demonstrate the accuracy of our asymptotic expansion by comparing results for the amplitude of the zeroth mode, $|R_0|$, with the exact solution for a cascade of finite-chord airfoils at zero incidence (the exact solution takes full account of the trailing edges, and has again been calculated using the prescription described by Peake 1993). In figure 4(*a*) we have $k = 10$, and kw runs from 4.7 at $M_\infty = 0.4$ to 32.9 at $M_\infty = 0.95$, and as can be seen exceedingly good agreement is obtained for Mach numbers larger than about 0.55. For the conditions considered in figure 4(*a*), as M_∞ is increased from zero the $n = 0$ mode becomes cut-on for $M_\infty > 0.35$, and the propagation direction approaches the shadow boundary $\theta(\zeta_{0s}^0) = \pi/2$ for $M \approx 0.85$. In the close vicinity of these two critical conditions, our asymptotic approximation breaks down as described above, and these regions have therefore not been plotted.

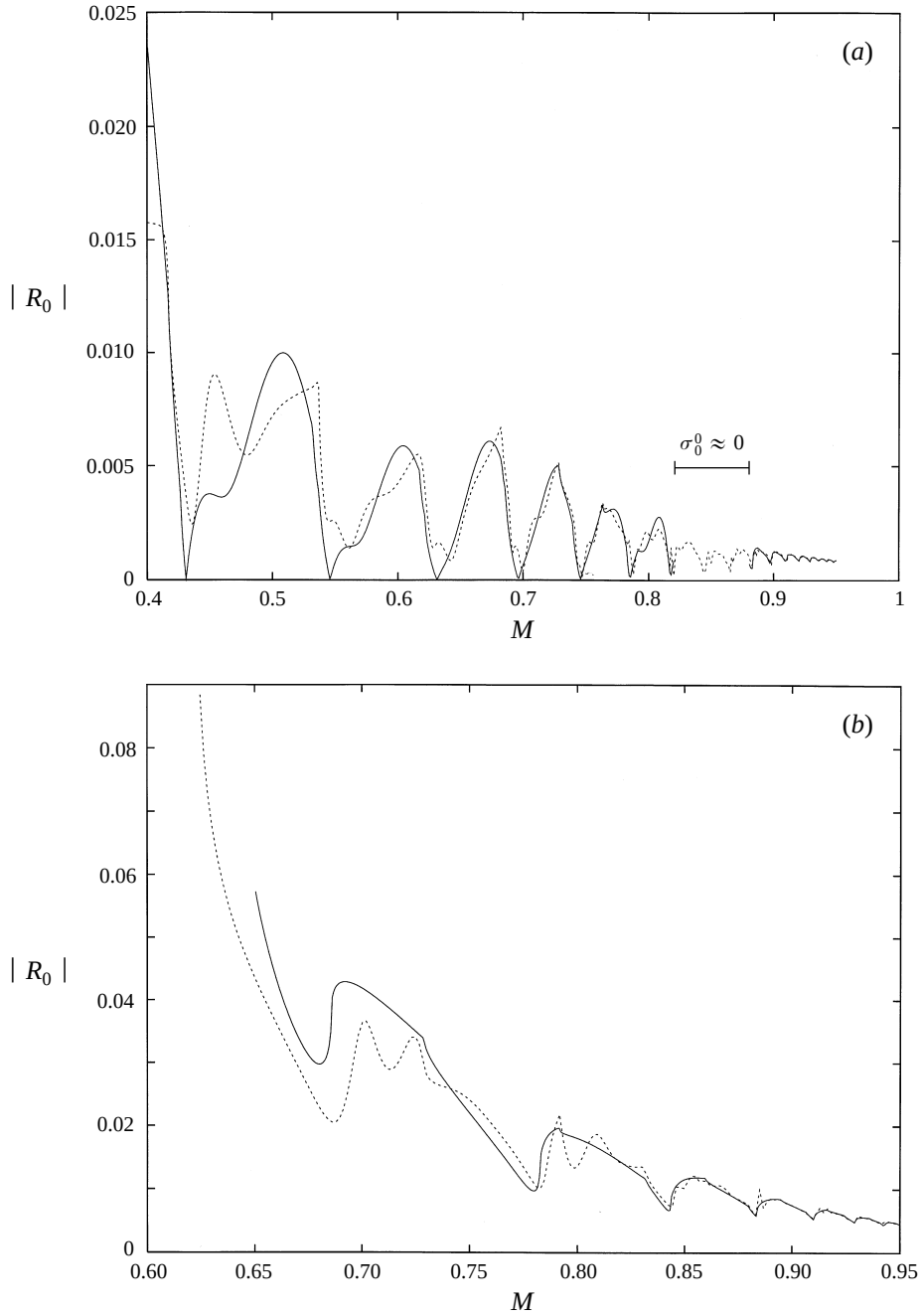

FIGURE 4. Plot of the amplitude of the $n = 0$ radiation mode as M_∞ is varied, calculated from an exact solution (dashed line) and the asymptotic solution described in §3 (solid line). Here $s_*/b_* = 2$, $d_*/b_* = 1$, $\sigma_0 = 2\pi$, $A_N = 1$ and (*a*) $k = 10$; (*b*) $k = 5$.

(As has already been mentioned, such non-uniformities could be handled using the sort of analysis described in Peake & Kerschen 1995*a*.) However, away from the non-uniformities our large-kw expansion is in good agreement with the exact solution. In figure 4(*b*) we use the smaller value $k = 5$ and here we have $4.3 < kw < 15.2$

as M_∞ is increased from 0.65 to 0.95, and even for this moderate value of k good agreement is obtained (here the $n = 0$ mode becomes cut-on at $M_\infty \approx 0.6$, explaining the discrepancy at the lower end of the M_∞ range). Finally, it should be emphasized that the mode index n used here to label our plane waves does not correspond to any mode number used to label the modes in a cylindrical duct (although the azimuthal mode number of a duct mode can of course be related to the number of blades in the blade row and to the inter-blade phase angle in our cascade); the connection between our two-dimensional cascade results and the acoustic field in a duct is described briefly in §6.

We have therefore established an accurate approximation for the case of zero blade incidence, in which the point of generation and subsequent propagation of each radiation component is explicitly identified. We can now go on to incorporate the non-uniform mean-flow effects arising from non-zero mean loading, and this will be described in the next two sections.

4. Steady flow for non-zero mean loading

In order to analyse the distortion of the incident gust and its subsequent interaction with the cascade, we first need to find the steady base flow through the cascade. Since $\delta \ll 1$, the steady-flow potential satisfies the usual linearized subsonic small-disturbance equation, and we make the Prandtl–Glauert transformation

$$x_*, y_* \rightarrow \phi_0, \psi_0, \tag{4.1}$$

and thereby convert the steady compressible flow through the cascade in physical space into an equivalent incompressible flow through a modified cascade in Prandtl–Glauert space. The Prandtl–Glauert transformation contracts distances perpendicular to the direction of the uniform base flow (here taken to be the upstream flow) by a factor β_∞, so that in the Prandtl–Glauert space the distance Δ_{pg} between leading edges is

$$\Delta_{pg} = \Delta_* \left(\cos^2(\alpha_* - \delta) + \beta_\infty^2 \sin^2(\alpha_* - \delta)\right)^{1/2} / b_*, \tag{4.2}$$

where non-dimensionalization by the blade semi-chord has also been incorporated in the transformation. In Prandtl–Glauert space, the front face of the cascade makes an angle

$$\alpha = \tan^{-1}[\beta_\infty \tan(\alpha_* - \delta)] \tag{4.3}$$

with respect to the positive ϕ_0-direction. Since we are only concerned with determining the steady flow to $O(\delta)$, we make the usual approximation of applying the normal-velocity boundary conditions not on the actual blade surfaces but instead on line segments parallel to the uniform base flow,

$$\psi_0 = n\Delta_{pg} \sin\alpha, \quad n\Delta_{pg} \cos\alpha < \phi_0 < n\Delta_{pg} \cos\alpha + 2, \quad n = 0, \pm 1, \pm 2 \ldots . \tag{4.4}$$

Expanding the complex potential as a perturbation series in δ, we have

$$\zeta \equiv \phi + \mathrm{i}\psi = \zeta_0 + \delta F(\zeta_0) + O(\delta^2) \tag{4.5}$$

where $\zeta_0 = \phi_0 + \mathrm{i}\psi_0 = (x_* + \mathrm{i}\beta_\infty y_*)/b_*$ is the (complex) independent variable in the Prandtl–Glauert space. Setting $F = \phi_1 + \mathrm{i}\psi_1$, the boundary condition on the blade surfaces then takes the form

$$\frac{\partial \phi_1}{\partial \psi_0} = -\frac{\partial \psi_1}{\partial \phi_0} = -\frac{1}{\beta_\infty} \tag{4.6}$$

on the line segments specified above. Equation (4.6) can be integrated to yield a simple expression for $\mathrm{Im}(F)$ on the blade surfaces. Note that the application of the Prandtl–Glauert transformation has introduced a factor β_∞^{-1} in the normal-velocity boundary condition, showing that the mean-flow disturbance for a blade deflection angle δ in the compressible stream corresponds to an equivalent incompressible flow for a blade deflection angle δ/β_∞. (The effective angle of attack δ/β_∞ differs from the distortion of the actual blade geometry under the Prandtl–Glauert transformation.) The (complex) disturbance velocity $F'(\zeta_0)$ is required to vanish at upstream infinity, and the Kutta condition is applied at the trailing edges. In §5, it will prove convenient that (4.6) provides a simple expression for ψ_1 on the blade surfaces, independent of the details of the cascade solution.

Thus, the determination of the steady flow has been reduced to the solution of an incompressible flow problem, which can be obtained using the theory of conformal mappings. Robinson & Laurmann (1956) and Thwaites (1960) describe the mapping of a circle onto our cascade of flat plates, which then provides an analytical, albeit implicit, expression for the complex potential $F(\zeta_0)$, and details are given in Appendix A. The quantity required for the analysis of the unsteady flow according to the formulation in §2 is $F(\zeta)$, requiring an inversion of (4.5), but since we neglect terms of $O(\delta^2)$, $F(\zeta_0)$ can be replaced by $F(\zeta)$ to the order of our analysis. In order to fix the arbitrary constant present in $F(\zeta)$, we suppose that F vanishes at the leading edge of blade 0, i.e. $F(0) = 0$. It then follows from the periodicity of the flow that $F = 0$ at each leading edge. The mean-flow perturbation decays exponentially with distance upstream of the cascade, and the complex potential F approaches a constant, $F(-\infty)$, as $\zeta \to \infty$ in the upstream region.

The cascade in physical space is mapped onto a cascade in ϕ, ψ space, with the blades being mapped onto lines parallel to the ϕ-axis. This new cascade has a stagger angle α and adjacent leading-edge separation $\Delta = \Delta_{pg}$ (see figure 5). The leading edge of blade n has position $n\Delta \exp(\mathrm{i}\alpha)$, and the leading edge and forward stagnation point can be taken as coincident, since their spacing is $O(\delta^2)$. It should be noted that the trailing edge of each blade is mapped onto two points in ϕ, ψ space, thanks to the non-zero circulation and consequent jump in the mean-flow velocity potential across each wake, but since, as has already been argued, the trailing edges have no effect at the asymptotic order considered, this difficulty is of no importance here.

It follows from the expression (2.6) for the gust that the inter-blade phase angle, σ, can be found in terms of the incident-gust wavenumbers as $\sigma = kd + kk_n s$, where $d = \Delta \cos\alpha$, $s = \Delta \sin\alpha$. For a mean flow which is an $O(\delta)$ perturbation about a uniform flow, Kerschen & Balsa (1981) have shown that the drift function, $g(\phi, \psi)$, representing the cumulative distortion of the vorticity and entropy gusts by the non-uniform steady flow as they are convected from upstream infinity, is given by

$$g(\phi, \psi) = -2\delta \mathrm{Re}[F(\zeta) - F(-\infty)] + O(\delta^2). \tag{4.7}$$

The drift experienced by the incident gust in travelling from infinity to the leading edge of each blade, denoted δg_l in order to expose the scaling on the small parameter δ, is then given by

$$\delta g_l = 2\delta \mathrm{Re}[F(-\infty)], \tag{4.8}$$

and an expression for $F(-\infty)$ follows from the conformal mapping. We note that δg_l is the same for each leading edge, as might be expected given the periodicity of the steady flow. For an isolated flat-plate airfoil at non-zero angle of attack the drift vanishes to leading order as can be seen by induced velocity arguments (see Myers &

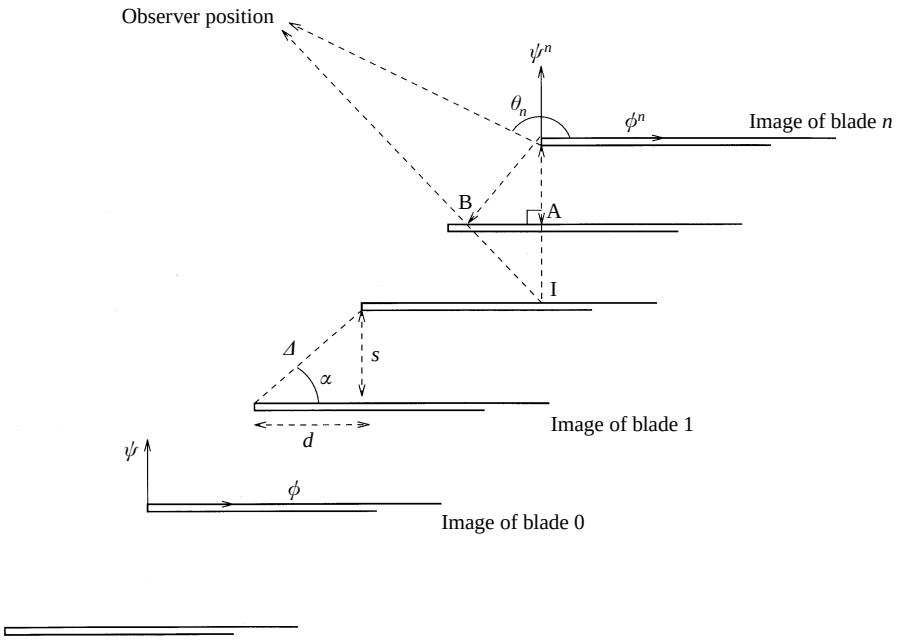

FIGURE 5. The image of the cascade in ϕ, ψ space.

Kerschen 1995), and this is also true for a cascade without stagger, but for a staggered cascade it turns out that $\delta g_l \neq 0$.

The form of the steady flow near each leading edge will be required for analysis of the unsteady flow, and in Appendix B it is shown that

$$F'(\zeta) \sim \frac{\delta_{eff}}{\beta_\infty}\left(\frac{2}{\zeta - n\Delta\exp(\mathrm{i}\alpha)}\right)^{1/2} \quad \text{as} \quad \zeta \to n\Delta\exp(\mathrm{i}\alpha), \tag{4.9}$$

where the parameter δ_{eff} is independent of n and has been determined from the conformal mapping. This square-root singularity is characteristic of the local mean-flow perturbation in the vicinity of each leading edge, and δ_{eff} is simply the effective incidence angle – i.e. (4.9) describes the flow near the leading edge of an *isolated* flat-plate airfoil inclined at an angle δ_{eff} to the oncoming stream. Since the cascade will act to turn the upstream flow so as to be aligned approximately along the blade chord, we expect that $\delta_{\mathrm{eff}} < \delta$, and this indeed turns out to be the case. This point is particularly significant, because it is essentially δ_{eff} which is the small parameter in our subsequent analysis of the sound-generation problem, and the range of validity of the asymptotic expansion is therefore likely to be larger than might at first be supposed. In what follows we write $\mathscr{C} \equiv \delta_{eff}/\delta$.

5. Unsteady flow for non-zero mean loading

5.1. *Local leading-edge analysis*

Myers & Kerschen (1995) demonstrate that the interaction between a high-frequency convected gust and an isolated airfoil can be treated using the method of matched asymptotic expansions, with an inner region around the leading edge scaling on the gust wavelength (so of size $O(k^{-1})$), and an outer region comprising the rest of space. An additional inner region is present around the trailing edge, together with a

transition region corresponding to the blade wake, but since we are only concerned with the forward-radiated noise here, these additional features can be neglected. In the outer region the mean flow varies slowly on the wavelength scale, and the incident gust convects along the mean-flow streamlines and is distorted according to (2.6). In the inner region around the leading edge, the lengthscale of the steady flow becomes comparable with the gust wavelength, and a complicated interaction between the steady and unsteady flows must occur, and sound is generated.

For our cascade problem, the local leading-edge analysis for each blade must be entirely equivalent to Myers & Kerschen's isolated-blade work, with the one proviso that the local mean-flow perturbation in the leading-edge region is given by (4.9), in which the parameter δ, which would have been present for the isolated airfoil, is replaced by δ_{eff} thanks to the turning effect of the cascade on the upstream flow. We therefore define sets of inner coordinates around each leading edge by

$$\Phi^n = (\phi - n\Delta\cos\alpha)k, \quad \Psi^n = (\psi - n\Delta\sin\alpha)k, \tag{5.1}$$

and write the modified unsteady velocity potential in the inner region around blade n in the form

$$H^n(\Phi^n, \Psi^n) = \frac{1}{k}[H_0 + \mathscr{C}\delta k^{1/2}(H_1 + H_2 + H_3) + O(\delta^2 k, \delta, 1/k)]. \tag{5.2}$$

Here the factor $\mathscr{C}$ has been introduced to account for the effective incidence angle at the leading edge. Substituting (5.2) into (2.11) and (2.13) and expanding for large k and small δ, the equations governing the local functions H_n are found to be identical to those appearing in Myers & Kerschen (1995), and the solutions developed there can be used directly. We note that the term H_0 is just the inner limit of the unsteady velocity potential for an airfoil at zero incidence, that H_1 accounts for the change in boundary conditions on the blade surface due to the distortion of the vortical gust, H_2 accounts for the quadrupole sources corresponding to Reynolds-stress fluctuations as well as distortion of the entropy gust, and H_3 accounts for the interaction between the zeroth-order sound field and the local mean flow.

Myers & Kerschen (1995) have shown that this inner solution matches onto a solution in the outer region which contains both convected and acoustical components, but since we are only interested in calculating the sound we consider here just the latter, which is shown to have modified velocity potential h of the form

$$\frac{D(\theta_n)\exp(\mathrm{i}kwr_n + \mathrm{i}k\delta P(r_n, \theta_n) + \mathrm{i}n\sigma' + \mathrm{i}k\delta g_l)}{k^{3/2}r_n^{1/2}}, \tag{5.3}$$

where r_n and θ_n are polar coordinates relative to the nth leading edge in ϕ, ψ space. The directivity $D(\theta)$ is given by

$$D(\theta) = \frac{A_N}{\beta_\infty}D_0(\theta, -1/\beta_\infty^2) + \mathscr{C}\delta k^{1/2}\,[D_1(\theta) + D_2(\theta) + D_3(\theta)] + O(\delta^2 k, \delta, 1/k), \tag{5.4}$$

and the complicated algebraic expressions for $D_{1,2,3}(\theta)$ are given by Myers & Kerschen (1995, equations 3.11*b*, 3.15*b–e*, 3.26*c*) and in Appendix C of this paper for completeness. The field spreads cylindrically from the leading edge, with a phase distortion due to the non-uniform mean flow given by the function

$$P(r_n, \theta_n) = V(\theta_n)Q(r_n, \theta_n), \tag{5.5}$$

where

$$V(\theta) = -\beta_\infty^2 w + \frac{(\gamma+1)M_\infty^4}{2\beta_\infty^2 w}\left(\frac{1}{\beta_\infty^2} - w\cos\theta\right)^2, \tag{5.6}$$

γ is the ratio of specific heats and

$$Q(r_n,\theta_n) \equiv \int_0^{r_n} q(r_n',\theta_n)\mathrm{d}r_n' = \mathrm{Re}\{\exp(-\mathrm{i}\theta_n)F(r_n\exp(\mathrm{i}\theta_n))\}. \tag{5.7}$$

The last step in (5.7) has been completed by noting that q is the real part of an analytic function. The modified inter-blade phase angle σ' is defined in (2.16) and (2.18). The final term in the phase in (5.3) arises from the distortion of the incident gust as it convects to the leading edge. By comparing (3.2) and (5.3), the effect of non-zero mean loading on the direct field (contribution (i) of §3) becomes clear, and we note in particular how the directivity is modified by an $O(\mathscr{C}\delta k^{1/2})$ amount, which although formally small will be significant for parameter values of practical interest. We also note, however, that the turning effect of the cascade on the upstream flow means that $\mathscr{C} < 1$, so that the effects of these additional sound sources in the leading-edge region will typically be somewhat smaller for a cascade than for an isolated airfoil. Even more significantly, the acoustic phase is modified by an $O(k\delta)$ amount, which is $O(1)$ in our preferred limit, and given the complicated phase interference effects between the different scattered radiation components which make up the forward-radiated noise, one would expect this phase change to have a very significant effect.

5.2. *Forward radiation*

The high-frequency cascade solution for non-zero δ is now developed following the same approach as in §3. In the high-frequency limit, the forward radiation consists of the four components illustrated in figure 2: (i) the direct field from each leading edge, (ii) the scattered field generated by the subsequent impingement of the direct field of a given blade on the leading edges of the other blades, (iii) the reflection of the direct field of a given leading edge by the blade below and its subsequent rescattering by the same leading edge, and (iv) the reflection of the direct field of a given blade off the blade below and its subsequent propagation to the far field.

The modifications to the direct field of a given blade n were discussed in the previous subsection. Here, we consider the reflection and scattering of this direct field by the other blades of the cascade. The non-uniform mean flow leads to $O(\delta k^{1/2})$ changes in the amplitude of the direct field (5.3) and $O(\delta k)$ changes to the phase. It is seen, however, that the orientation of a surface of constant phase is modified only by an $O(\delta)$ amount. In this paper we are only concerned with the $O(\delta k^{1/2})$ and $O(\delta k)$ corrections to the radiation directivity and phase, so that in considering the reflection and scattering of the direct field of a given blade by other blades, the local orientations of the incident and reflected rays can be approximated by their values for the case $\delta = 0$. Also, since the blade surfaces are flat, the Cauchy Riemann conditions show that $\partial q/\partial\psi$ vanishes on the blade surfaces, so that (2.13) reduces to $\partial h/\partial\psi = 0$ for the acoustic component of the field. Thus, the construction of the ray paths and image representations for the scattering and reflection processes when δ is non-zero is exactly the same as for the $\delta = 0$ case in §3, but the amplitude along a given ray path is modified due to the $O(\delta k^{1/2})$ amplitude correction to the direct field, and the phase along the ray is modified due to the $O(\delta k)$ influence of the mean-flow perturbation.

The $O(k\delta)$ corrections to the phases of the four radiation components are calculated separately.

(i) The direct field generated at the leading edge of blade n is now given by (5.3). The phase distortion (relative to the case $\delta = 0$) suffered by this radiation as it propagates from the leading edge of blade n directly to the far field is found to be

$$k\delta P(\infty, \theta_n) \equiv k\delta p_1 = k\delta V(\theta_n)\mathrm{Re}\{\exp(-\mathrm{i}\theta_n)F(-\infty)\}. \tag{5.8}$$

Note that, in the upstream direction $\alpha < \theta_n < \pi + \alpha$, the mean-flow disturbance potential $F(r_n \exp(\mathrm{i}\theta_n))$ approaches a constant value, $F(-\infty)$, which is independent of θ_n as $r_n \to \infty$.

(ii) The direct field from the leading edge of blade n interacts with all the other leading edges in exactly the same way as described in §3. The phase distortion experienced by the direct field from blade n as it travels to the leading edge of blade $n + m$ is $k\delta P(m\Delta, \alpha)$ for $m > 0$ and $k\delta P(-m\Delta, \pi + \alpha)$ for $m < 0$, and both these quantities are identically zero thanks to the fact that F vanishes at each leading edge. (The fact that F vanishes at each leading edge leads to $Q(\Delta, \alpha) = 0$ from (5.7), and this is a consequence of mass conservation; the total mass flux into the cascade between each blade must be the same as that between adjacent stagnation streamlines at upstream infinity, so that the perturbation mass flux at the cascade, $Q(\Delta, \alpha)$, must be zero.)

(iii) The radiation emitted in the negative ψ-direction by the leading edge of blade n is reflected by blade $n - 1$ and then rescattered by the leading edge of blade n, and this process of reflection and rescattering continues indefinitely. The repeated phase distortions which these waves experience in this process are calculated as follows. First, generalizing the result (5.5), the phase distortion due to non-uniform mean-flow effects in the propagation of an acoustic wave from point $\zeta_a = \phi_a + \mathrm{i}\psi_a$ to point $\zeta_b = \phi_b + \mathrm{i}\psi_b$ is

$$k\delta P_1(\zeta_b, \zeta_a) = k\delta V(\theta)\mathrm{Re}\{\exp(-\mathrm{i}\theta)(F(\zeta_b) - F(\zeta_a))\}, \tag{5.9}$$

where θ is the angle between the line segment from ζ_a to ζ_b and the positive ϕ-direction. The phase distortion in propagating from the leading edge of blade n to the point of reflection A on blade $n - 1$ (see figure 5) is then $k\delta P_1(-\mathrm{i}s, 0) = k\delta P(s, 3\pi/2)$, while the phase distortion on the return path to the leading edge of blade n is given by $k\delta P_1(0, -\mathrm{i}s)$. (Here the locations ζ_a and ζ_b have been expressed in coordinates referenced to the leading edge of blade n.) Combining these results, the total phase distortion which occurs in one cycle around the path from the leading edge of blade n to point A and back is

$$k\delta p_2 = -k\delta 2V(\pi/2)\mathrm{Im}\{F(-\mathrm{i}s)\}, \tag{5.10}$$

where we have used the result that $V(\theta) = V(2\pi - \theta)$. As noted in §4, the value of $\mathrm{Im}\{F\}$ on the blade surfaces is easily determined from the boundary condition (4.6) which the mean-flow perturbation satisfies. The point A on blade $n - 1$ is a distance d from the leading edge, so that $\mathrm{Im}\{F(-\mathrm{i}s)\} = d/\beta_\infty$ and

$$p_2 = -2V(\pi/2)\Delta\cos(\alpha)/\beta_\infty. \tag{5.11}$$

(iv) The radiation emitted from the leading edge of blade n in directions $\pi/2 < \theta_n < \pi - \alpha$ is reflected by blade $n - 1$ before reaching the far field, and the phase distortion associated with this can be calculated in very much the same way as described in (iii) above. The phase distortion in propagating from the leading edge of blade n to point B on the upper surface of blade $n - 1$ is given by $k\delta P_1(\zeta_B, 0)$,

while the phase distortion on the reflected path extending out to the far field is $k\delta P_1(\zeta_\infty, \zeta_B)$. Combining these two contributions, the total phase distortion along the path reflecting off point B and extending to the far field is $k\delta(p_1 + p_3)$, where

$$\begin{aligned} p_3 &= -2V(\theta_n)\sin\theta_n \mathrm{Im}\{F(\zeta_B)\} \\ &= -2V(\theta_n)\Delta\sin(\alpha+\theta_n)/\beta_\infty \end{aligned} \tag{5.12}$$

and the second step of (5.12) has been completed using the fact that the distance from the leading edge of blade $n-1$ to point B is $s(\cot\alpha + \cot\theta_n)$. We notice that when $\theta_n + \alpha = \pi$ (corresponding to the reflection point B lying exactly at the leading edge of blade $n-1$) then $p_3 = 0$, which is entirely to be expected since from (ii) the distortion associated with propagating between leading edges is exactly zero.

The total radiation falling on the leading edge of blade n is therefore found by adding together contributions (ii) and (iii) in exactly the same way as before. The corresponding velocity potential is then just given by a modified version of (3.4), in which all the quantities with suffix $_0$ are replaced by the corresponding quantity for $\delta \neq 0$, and in particular $B_0^{1,2,3} \to B^{1,2,3}$, with

$$\left.\begin{aligned} B^1 &= \sum_{m=1}^{\infty}\left\{\frac{D(\pi+\alpha)\exp(\mathrm{i}kwm\Delta + \mathrm{i}m\sigma' + \mathrm{i}k\delta g_l)}{m^{3/2}\Delta^{1/2}}\right\} \\ B^2 &= \sum_{m=1}^{\infty}\left\{\frac{D(\alpha)\exp(\mathrm{i}kwm\Delta - \mathrm{i}m\sigma' + \mathrm{i}k\delta g_l)}{m^{3/2}\Delta^{1/2}}\right\} \\ B^3 &= \sum_{m=1}^{\infty}\left\{\frac{D(3\pi/2)\exp(2\mathrm{i}kwms + \mathrm{i}k\delta m p_2 + \mathrm{i}k\delta g_l)}{m^{3/2}(2s)^{1/2}}\right\}. \end{aligned}\right\} \tag{5.13}$$

Note the inclusion of the phase factor $\exp(\mathrm{i}k\delta m p_2)$ in the last term to account for the refractive effects in the multiple reflection associated with contribution (iii).

When this radiation interacts with the leading edge of blade n, the resulting upstream radiation can be thought of as being composed of two components. One component is equal to the upstream radiation produced in the scattering by an edge in uniform flow (i.e. as if $\delta = 0$), with a velocity potential of size $O(k^{-2})$; and the second component is a correction to account for the sound generated by the interaction of the incident radiation and the local mean-flow disturbance in the leading-edge region, with a velocity potential of size $O(k^{-3/2}\delta)$. This correction is smaller than either of the first two terms in our expansion of the directivity of the forward radiation, and the effects of $\delta \neq 0$ can therefore be neglected in the local rescattering process. It follows that the unsteady velocity potential upstream of the cascade due to the direct field of blade n and the rescattering at the leading edge of blade n, but excluding contribution (iv) for the moment, can be found by modification of (3.6) in the form

$$\begin{aligned} f^n(\phi^n, \psi^n) = \frac{\exp(\mathrm{i}kwr_n + \mathrm{i}k\delta p_1 + \mathrm{i}n\sigma')}{k^{3/2}r_n^{1/2}}\Bigg\{ & D(\theta_n)\exp(\mathrm{i}k\delta g_l) - \frac{\mathrm{i}B^1 w\sin\alpha}{k^{1/2}}D_0(\theta_n, w\cos\alpha) \\ & + \frac{\mathrm{i}wB^2\sin\alpha}{k^{1/2}}D_0(\theta_n, -w\cos\alpha) + \frac{\mathrm{i}wB^3}{k^{1/2}}D_0(\theta_n, 0)\Bigg\}. \end{aligned} \tag{5.14}$$

Summing over the blade index n and including the reflected contribution (iv), we find

that the total unsteady velocity potential ahead of the cascade is

$$h(\phi,\psi)=\sum_{n=-\infty}^{\infty}\left[f^n(\phi^n,\psi^n)+f^n(\phi^n,-\psi^n-2s)\exp(\mathrm{i}k\delta p_3)\{\mathrm{H}(\theta_n-\pi/2)-\mathrm{H}(\theta_n-\pi+\alpha)\}\right]. \tag{5.15}$$

Note that the use of the image-source construction here has already been fully justified at the beginning of §5.2.

Finally, the summation over the blade index n in (5.15) is converted to a summation over the upstream mode index by the same method as utilized in §3.2. By suitable modification of (3.18), we find that the modified unsteady velocity potential takes the form

$$\sum_{n=-r}^{q} R_n(\theta(\zeta_s^n))\exp(-\mathrm{i}\sigma^n\phi-\mathrm{i}\eta^n\psi) \tag{5.16}$$

far upstream, where

$$R_n(\theta)=\mathscr{R}_n(\theta)+\mathscr{R}_n(2\pi-\theta)\exp(-2\mathrm{i}s\eta^n+\mathrm{i}k\delta p_3)\{\mathrm{H}(\theta-\pi/2)-\mathrm{H}(\theta-\pi+\alpha)\} \tag{5.17}$$

and

$$\mathscr{R}_n(\theta)=\frac{\exp(\mathrm{i}\pi/4)(2\pi)^{1/2}w^{\frac{1}{2}}\exp(\mathrm{i}k\delta p_1)}{k\left[\Delta^2k^2w^2-(2n\pi-\sigma')^2\right]^{1/2}}\left[D(\theta)\exp(\mathrm{i}k\delta g_l)-\frac{\mathrm{i}B^1w\sin\alpha}{k^{1/2}}D_0(\theta,w\cos\alpha)\right.$$
$$\left.+\frac{\mathrm{i}B^2w\sin\alpha}{k^{1/2}}D_0(\theta,-w\cos\alpha)+\frac{\mathrm{i}B^3w}{k^{1/2}}D_0(\theta,0)\right]. \tag{5.18}$$

We note that since $D(\theta)\neq D(2\pi-\theta)$, it is not possible to simplify (5.18) in the same way as was possible for (3.19) when $\delta=0$. The new saddle point ζ_s^n and the modal wavenumbers σ^n and η^n are obtained simply by replacing $\sigma_0', \Delta_0, \alpha_0$ by σ', Δ, α in (3.14) and (3.17) respectively; for instance,

$$\left.\begin{aligned}\sigma^n &= [(2n\pi-\sigma')\cos\alpha+\sin\alpha(\Delta^2k^2w^2-(2n\pi-\sigma')^2)^{1/2}]/\Delta,\\ \eta^n &= [(2n\pi-\sigma')\sin\alpha-\cos\alpha(\Delta^2k^2w^2-(2n\pi-\sigma')^2)^{1/2}]/\Delta,\end{aligned}\right\} \tag{5.19}$$

which are now cut-on for $-r\leqslant n\leqslant q$. It is clear that mean loading modifies the modal amplitudes, but the variation of the wavenumbers (5.19) as δ is increased depends on the precise way in which the cascade geometry is adjusted. If one considers precisely the same cascade throughout (i.e. keep the stagger α_* fixed) and then rotates the whole cascade clockwise about the midpoint of blade 0 (so that the angle to the upstream flow direction, δ, is increased) then it is certainly the case that the wavenumbers, and therefore the number which are cut-on, change. In fact, Δ increases and α decreases if δ is increased with α_* fixed, but the variation of σ' is more complicated and depends on the relative size of α and the gust transverse wavnumber k_n. Alternatively, however, if one keeps the line of leading edges fixed and then increases the angle between the blades and this fixed line, so that both δ and α_* are increased but the difference $\alpha_*-\delta$ remains the same, then it follows that the wavenumbers are unchanged from their unloaded values, since it is only $\alpha_*-\delta$, and not α_* or δ individually, which appears in (5.19) (see (4.2) and (4.3)). We also note that it is the modified inter-blade phase angle σ', and not the gust inter-blade phase angle σ, which appears in (5.19), and this is due to the presence of the non-zero uniform flow upstream, and arises mathematically from the Miles transformation (2.10). The difference between σ and σ' can therefore be attributed to a Doppler effect (actually $\sigma'-\sigma=kM_\infty^2d/\beta_\infty^2$), and we note that this

again depends on the angle $\alpha_* - \delta$, and therefore does not change from its unloaded value as δ is increased with the line of leading edges held fixed.

Equation (5.18) becomes singular, and is therefore invalid, at certain critical conditions, in exactly the same way as was (3.16) for $\delta = 0$. Just as before, these non-uniformities occur when $\sigma^n = \pm kw\cos\alpha$, corresponding to the cut-on conditions of the mode n and the shadow-boundary non-uniformity at $\theta = \pi - \alpha$, and also when $\sigma^n = 0$ (for which just the last term in (5.18) is singular, corresponding to coincidence with the shadow-boundary non-uniformity in our expression for $D_0(\theta, 0)$). Finally, by considering the behaviour of $\phi + \mathrm{i}\psi$ at upstream infinity it follows that we can rewrite equation (5.16) in terms of the physical coordinates, to give the upstream unsteady velocity potential as

$$\sum_{n=-r}^{q} R_n(\theta(\zeta_s^n))\exp(-\mathrm{i}\sigma^n \mathrm{Re}[\delta F(-\infty)] - \mathrm{i}\eta^n \mathrm{Im}[\delta F(-\infty)])\exp\left(-\mathrm{i}\sigma^n x_*/b_* - \mathrm{i}\eta^n \beta_\infty y_*/b_*\right). \tag{5.20}$$

5.3. *Sample results*

Here we consider for simplicity just two-dimensional purely vortical gusts, so that $A_z = k_z = B = 0$. In figure 6 we demonstrate the large effect that even a relatively modest level of mean loading can have on the forward-radiated noise, by comparing the amplitude of the $n = 1$ mode for zero mean loading ($\delta = 0$) with results calculated using the above asymptotic theory for $\delta = 0.25$. For the cascade considered in figure 6, the factor $\mathscr{C}$ relating δ and δ_{eff} is $\mathscr{C} = 0.41$ and $F(-\infty) = 0.15 + \mathrm{i}0.61$; the small parameter $\mathscr{C}\delta k^{1/2}$ in (5.4) therefore ranges over $0.25 < \mathscr{C}\delta k^{1/2} < 0.46$. As can be seen, the mean loading leads to significant change in $|R_1|$, shifting the locations of the maxima and minima and increasing the amplitude by more than a factor 2. The sharp local turning points observed on both curves are characteristic of cascade noise, and appear as successively higher-order modes become cut-on for increasing k. The mean loading has been introduced by rotating the cascade by an angle δ about the leading edge of blade 0 while holding the physical stagger angle α_* constant, and therefore the mean loading has caused a shift in the cut-on frequencies. We also note that while the amplitude of the $n = 1$ upstream mode for the unloaded cascade becomes zero for various values of k, the mode amplitude for the loaded cascade remains strictly positive. This can be explained by noting from (3.19) that for $\delta = 0$ the zeros of $|R_1|$ seen in figure 6 occur when $\exp(-2\mathrm{i}s_0\eta_0^1) = 1$; in this situation the source at each leading edge and its image in the lower blade produce radiation which, in the propagation direction associated with the $n = 1$ mode, is exactly out of phase and interferes destructively leading to a zero amplitude for this mode. When $\delta \neq 0$, however, this total destructive interference no longers occurs for these parameter values, because the radiation from the source and its image experience different phase distortions as they propagate to the far field. In addition, when mean loading is introduced, $D(\theta)$ is no longer antisymmetric ($D(\theta) \neq -D(2\pi - \theta)$), ruling out the possibility of total destructive interference at other angles. In figure 7, we plot the amplitude $|R_1|$ of the $n = 1$ mode against δ for the case $k = 10$, and as would be expected the effects of mean loading become increasingly strong as δ is increased from zero. For the parameter values chosen, we find that $\sigma^1 \approx 0$ for $\delta \approx 0.13$, so that our asymptotic approximation becomes invalid, and a small neighbourhood in the vicinity of this point is therefore excluded.

There are essentially three different effects which contribute to the substantial dif-

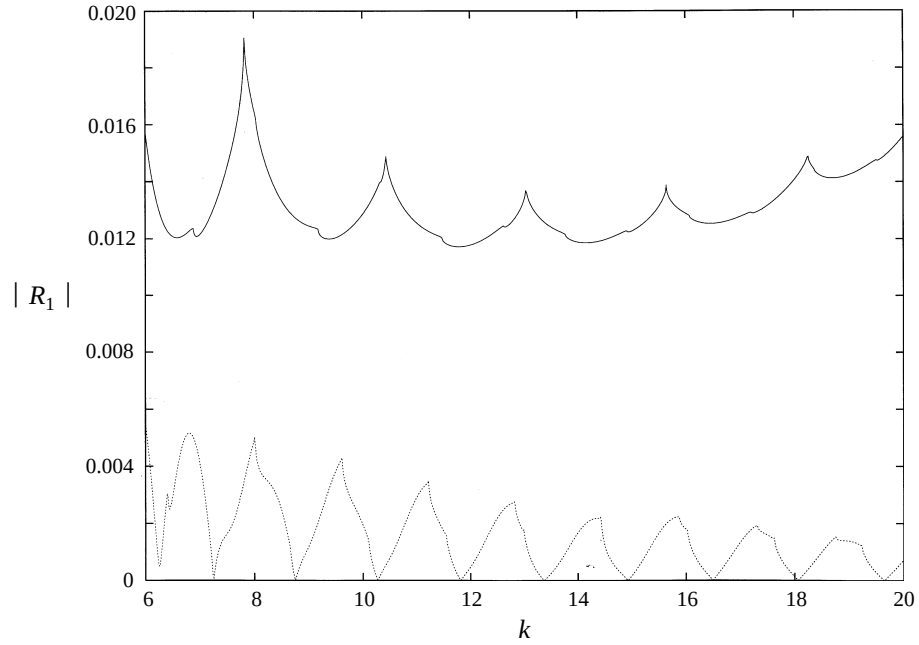

FIGURE 6. Plot of the amplitude $|R_1|$ of the $n = 1$ radiation mode for varying reduced frequency k. Here, $s_*/b_* = 2$, $d_*/b_* = 1$, $M_\infty = 0.7$, $A_N = 1$, $A_t = A_z = k_z = 0$ and $B = 0$, and $\delta = 0.25$ (solid line), $\delta = 0$ (dashed line).

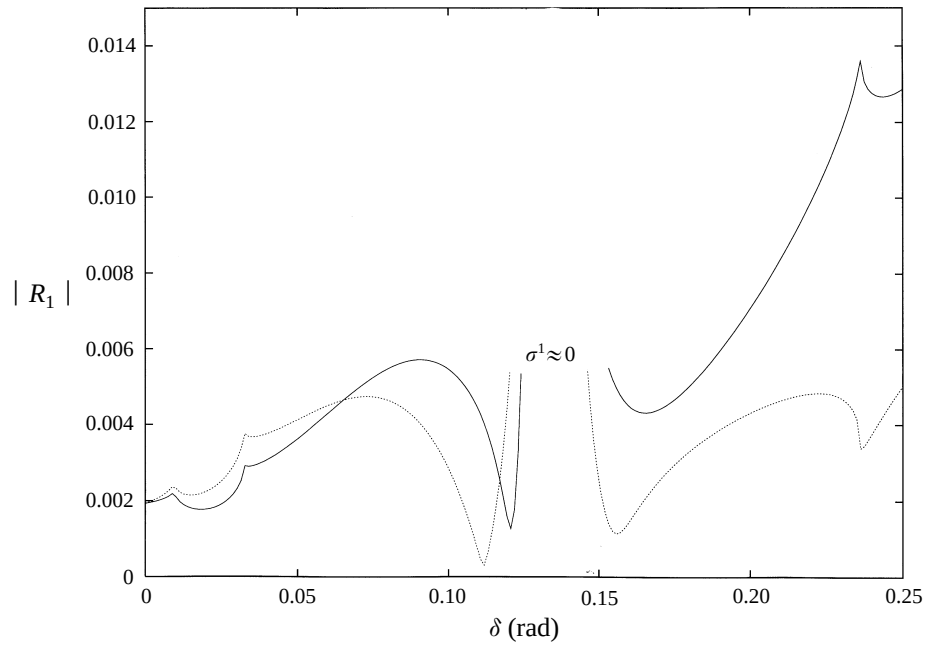

FIGURE 7. Plot of the amplitude $|R_1|$ of the $n = 1$ radiation mode as a function of angle of attack, δ (solid line). Here $k = 10$, with other conditions as in figure 6. The dashed line represents the total radiation minus the component generated by the action of the mean-loading related sources at each leading edge.

ferences between the values of $|R_1|$ for loaded and unloaded cascades which were illustrated in figures 6 and 7. First, the effective cascade stagger angle α and leading-edge separation Δ are functions of the inclination of the front face of the cascade to the oncoming stream, and therefore depend on the loading (in fact, α and Δ differ from their $\delta = 0$ values by $O(\delta)$). We can estimate the effect of this modification by considering the substitution $\alpha_0 \to \alpha$, $\Delta_0 \to \Delta$ in (3.15), from which it becomes clear that the phases of each of the various radiation components change by an $O(k\delta)$ amount, while the amplitudes are changed by a small amount of relative size $O(\delta)$. Second, the various radiation components experience a phase distortion of size $O(\delta k)$ in propagating through the non-uniform flow. Third, extra noise is generated at each leading edge by the additional source mechanisms associated with the local mean-flow gradients (i.e. the second set of terms in (5.4)), and the amplitude of this radiation is smaller than that produced by the force-dipole distribution of the unloaded cascade (i.e. the first term in (5.4)) by a factor of size $O(\delta k^{1/2})$. It is clear that the first and second effects will certainly make a significant contribution, since the associated phase changes are $O(1)$ in our preferred limit, but it might be thought that the third effect is much less important, since it only produces radiation of formally small relative amplitude $O(\delta k^{1/2})$. For typical values of k and δ, however, these additional source mechanisms make a significant contribution, and this is demonstrated in figure 7, where we present a plot of the total upstream radiation minus the contribution from the mean-loading-related leading-edge sources (which is completed in our analysis by simply setting $\mathscr{C} = 0$). The discrepancy between the two curves is certainly non-trivial for realistic values of δ greater than about 0.15, illustrating the importance of the mean-loading-related sources in the vicinity of the leading edges which were originally analysed by Myers & Kerschen (1995).

6. Concluding remarks

In this paper we have described the derivation of a consistent asymptotic approximation for the forward radiation generated by the interaction between convected disturbances and a cascade of loaded flat-plate airfoils. At the high frequencies considered, the noise is generated in small regions around the blade leading edges, and is then diffracted by the leading edges of all the other blades in the cascade, reflected by the adjacent blades, and refracted as it propagates through the non-uniform flow. In physical terms, the effects of mean loading are essentially two-fold. First, the mean-flow distortion leads to additional sound sources at each leading edge of relative amplitude $O(\delta k^{1/2})$, which will be significant for typical values of k and δ found in practice. Second, $O(1)$ phase changes are induced in the various radiation components as they propagate through the non-uniform mean flow, and given the strong interference effects present in cascade noise, this modification also gives rise to an important effect.

Once the calculations described in this paper have been completed, it is worth mentioning here how they can be used directly in a noise prediction scheme. One approach will be to use our cascade results to calculate the radiation modes at each radius along the span, as is done in strip theory, and then to use this information as initial data in ray tracing to calculate the acoustic field in the cylindrical duct ahead of the blade row. We note that the ray description of cylindrical duct modes given by Chapman (1994) will be particularly useful in this regard. It is significant here that our theory has been developed for the general case of three-dimensional incident gusts, and hence can be used to calculate the generation of acoustic waves with non-zero radial wavenumber. A second possibility is to use the approach described in this paper to calculate the blade lift (the precise analysis will be described in a

later paper) which can then be used as the source term in a rotating-source radiation integral for the resulting noise.

Work is now progressing on incorporating the effects of blade camber and thickness into calculating the unsteady lift distribution on the blades, and into developing expansions valid close to the non-uniformities described in §3, using the same approach as has been employed here. When this is complete, we believe that our analysis will provide a comprehensive prediction scheme for unsteady cascade flow, as well as providing very considerable insight into the underlying physics of the problem.

The authors gratefully acknowledge the financial support provided by the Royal Society and the Nuffield Foundation (N.P.) and NASA under grant NAG3-1442 (E.J.K.), and the assistance of Ingmar Evers in obtaining certain numerical results.

Appendix A

In this Appendix we describe the conformal mapping which is used to determine the steady flow through the cascade. This result is described more fully by Robinson & Laurmann (1956, p. 149ff), but we include it here in terms of the notation used in this paper for completeness. In the ζ_0 (Prandtl–Glauert)-plane the flow is incompressible and the cascade geometry is as shown in figure 1, but with the blades inclined at an angle δ/β_∞ to the upstream mean flow, stagger angle $\alpha_{pg} = \alpha + \delta/\beta_\infty$, leading-edge spacing Δ_{pg} and chord length 2. A conformal mapping of a circle of radius a in the η -plane onto this cascade in the ζ_0-plane is given by

$$\exp(\mathrm{i}\delta/\beta_\infty)\zeta_0 - 1 = \frac{\Delta_{pg}}{2\pi}\left\{\exp(+\mathrm{i}\alpha_{pg} - \mathrm{i}\pi/2)\log\left(\frac{b+\eta}{b-\eta}\right) + \exp(-\mathrm{i}\alpha_{pg} + \mathrm{i}\pi/2)\log\left(\frac{\eta + a^2/b}{\eta - a^2/b}\right)\right\}; \quad \text{(A 1)}$$

note the origin and orientation of the axes differs from those used in Robinson & Laurmann (1956). The ratio b/a (> 1) is found as the solution of an implicit equation derived by noting that the circle is mapped onto blades of chord length 2; this equation turns out to be

$$2 = \frac{2\Delta_{pg}}{\pi}\left\{\sin\alpha_{pg}\log\left(\frac{(\cosh^2\log(b/a) - \cos^2\alpha_{pg})^{1/2} + \sin\alpha_{pg}}{\sinh[\log(b/a)]}\right) + \cos\alpha_{pg}\tan^{-1}\left(\frac{\cos\alpha_{pg}}{[\cosh^2\log(b/a) - \cos^2\alpha_{pg}]^{1/2}}\right)\right\} \quad \text{(A 2)}$$

(note the typographical error in Robinson & Laurmann, p. 151 equation 2.11,14), and can be solved numerically for b/a in a straightforward manner. The non-dimensional perturbation potential, $\delta F(\zeta_0)$, for the incompressible flow through the cascade in the ζ_0-plane can then be written down as

$$\delta F(\zeta_0) = \frac{U_m\Delta_{pg}}{2\pi U_\infty}\left\{\exp(-\mathrm{i}\iota_m)\log\left(\frac{b+\eta}{b-\eta}\right) + \exp(\mathrm{i}\iota_m)\log\left(\frac{\eta + a^2/b}{\eta - a^2/b}\right)\right\} - \frac{\mathrm{i}\Gamma}{4\pi}\log\left\{\frac{\eta^2 - a^4/b^2}{\eta^2 - b^2}\right\} - \frac{\Delta_{pg}\exp(-\mathrm{i}\delta/\beta_\infty)}{2\pi}\left\{\exp(+\mathrm{i}\alpha_{pg} - \mathrm{i}\pi/2)\log\left(\frac{b+\eta}{b-\eta}\right) + \exp(-\mathrm{i}\alpha_{pg} + \mathrm{i}\pi/2)\log\left(\frac{\eta + a^2/b}{\eta - a^2/b}\right)\right\} + C, \quad \text{(A 3)}$$

where the arbitrary constant C is chosen so that δF vanishes at $\zeta_0 = 0$, Γ is the circulation, U_m is the modulus of the average of the uniform flow velocities far upstream and far downstream of the cascade, and ι_m is the angle between this average velocity and the normal to the front face of the cascade in Prandtl–Glauert space. The extra factor δ in the definition of the perturbation potential will prove convenient in subsequent asymptotic analysis; by analogy with the flow round an isolated blade, it is easy to see that $\delta F = O(\delta)$ for $\delta \ll 1$. It now follows that

$$\tan \iota_m = (\tan \iota_1 + \tan \iota_2)/2, \tag{A 4}$$

where $\iota_{1,2}$ are the angles between the upstream and downstream flows and the front face of the cascade in Prandtl–Glauert space (see figure 1), and this downstream angle is found from the relation

$$\tan \iota_2 = \frac{Q \tan \iota_1 + 2 \cot \alpha_{pg}}{Q + 2}, \tag{A 5}$$

where

$$Q = \frac{(\cosh^2(\log(b/a)) - \cos^2 \alpha_{pg})^{1/2}}{\sin \alpha_{pg}} - 1. \tag{A 6}$$

The mean velocity U_m can be determined simply from mass conservation, and satisfies

$$U_m \cos \iota_m = U_\infty \cos \iota_1. \tag{A 7}$$

We are now able to calculate the circulation, using

$$\Gamma = \frac{2\Delta_{pg} U_m \cos(\iota_m + \alpha_{pg})}{[\cosh^2(\log(b/a)) - \cos^2 \alpha_{pg}]^{1/2}}, \tag{A 8}$$

and the steady incompressible flow through the cascade in the ζ_0-plane is thereby completely specified (typically $\Gamma < 0$).

Finally, we note that the point $\eta = -b$ maps onto the point at upstream infinity in the ζ_0-plane, and the points $\eta_{l,t} = a \exp(\mathrm{i}\theta_{l,t})$ map onto the leading edge and trailing edge, where $\theta_{l,t}$ are solutions of

$$\tan \theta = \tanh[\log(b/a)] \cot \alpha_{pg}, \tag{A 9}$$

with $\theta_l > \pi$ and $\theta_t = \theta_l - \pi$. The upper and lower surfaces of the blade are then obtained by moving along the circle $|\eta| = a$ from $a \exp(\mathrm{i}\theta_l)$ towards $a \exp(\mathrm{i}\theta_t)$ in the clockwise and anticlockwise directions respectively. Since the factor $\log(\eta^2 - a^4/b^2)$ in the circulation term in (A 3) is multi-valued as one moves along the circle $|\eta| = a$, the complex potential at the trailing edge takes two values, depending on whether one has approached it along either the upper or the lower blade surface. In fact, it is easy to see from (A 3) that the imaginary parts of the complex potentials at the trailing edge are equal, but that the real part corresponding to the upper surface is greater than that corresponding to the lower surface by $-\Gamma$; this is entirely to be expected, since the flow must accelerate over the upper (suction) surface of each blade.

The quantities $\mathscr{C}$ and $F(-\infty)$, which are required for our acoustic calculations, can now easily be determined.

Appendix B

In this Appendix we use the conformal mapping stated above to analyse the form of the steady flow in the vicinity of the blade leading edges. We note first that close

to the nth leading edge $\zeta_0 = n\Delta_{pg}\exp(\mathrm{i}\alpha)$ we have

$$\zeta_0(\eta) \approx n\Delta_{pg}\exp(\mathrm{i}\alpha) + \tfrac{1}{2}(\eta-\eta_l)^2\frac{\mathrm{d}^2\zeta_0}{\mathrm{d}\eta^2}_{\eta=\eta_l} \tag{B 1}$$

where the point $\eta = \eta_l$ maps onto the leading edges, and where we have used the fact that $\mathrm{d}\zeta_0/\mathrm{d}\eta = 0$ at the blade edges. We now use

$$\frac{\mathrm{d}F}{\mathrm{d}\zeta_0} = \frac{\mathrm{d}F}{\mathrm{d}\eta}\left(\frac{\mathrm{d}\zeta_0}{\mathrm{d}\eta}\right)^{-1}, \tag{B 2}$$

and it follows that

$$\frac{\mathrm{d}F}{\mathrm{d}\zeta_0} \approx \left\{\frac{\mathrm{d}F/\mathrm{d}\eta}{2\left[\mathrm{d}^2\zeta_0/\mathrm{d}\eta^2\right]^{1/2}}\right\}_{\eta=\eta_l}\left(\frac{2}{\zeta_0 - n\Delta_{pg}\exp(\mathrm{i}\alpha)}\right)^{1/2}. \tag{B 3}$$

The quantity in curly brackets is the effective incidence angle, $\delta_{eff}/\beta_\infty$, at each leading edge, and the various quantities in (B 3) can easily be evaluated from Appendix A.

Appendix C

In this Appendix we present, for completeness, the expressions for the leading-edge directivity function, $D(\theta)$, derived by Myers & Kerschen (1995). From (5.4) we see that $D(\theta)$ is written as a linear combination of four functions $D_0(\theta, -1/\beta_\infty^2)$ and $D_{1-3}(\theta)$. An expression for D_0 is already given in this paper in (3.3), and we merely quote the remaining results as follows:

$$D_1(\theta) = \frac{2\mathrm{i}A_N\beta_\infty^{-2}}{w^{1/2}(\beta_\infty^{-2} - w\cos\theta)^{3/2}}. \tag{C 1}$$

$$D_2(\theta) = D_{2p}(\theta) + D_{2c}(\theta), \tag{C 2}$$

where

$$D_{2p}(\theta) = \frac{-\mathrm{i}(\beta_\infty^{-2} - w\cos\theta)f_1(-w\cos\theta) + k_n f_2(-w\cos\theta)}{4(\beta_\infty^{-4} + k_n^2)[2w(\beta_\infty^{-2} - w\cos\theta)]^{1/2}(\lambda_1 + w\cos\theta)(\lambda_2 + w\cos\theta)}, \tag{C 3}$$

$$\begin{aligned} D_{2c}(\theta) = -\Bigg[&4(\lambda_1-\lambda_2)(\mathrm{i}k_nC_4 + \mathrm{i}\beta_\infty^{-2}C_3) + \frac{(\lambda_1+w)^{1/2}f_2(\lambda_1)}{(\lambda_1+\beta_\infty^{-2})^{1/2}(\lambda_1+w\cos\theta)} \\ &- \frac{(\lambda_2+\beta_\infty^{-2})f_2(\lambda_2) + \mathrm{i}k_nf_1(\lambda_2)}{[(\lambda_2-w)(\lambda_2+\beta_\infty^{-2\prime})]^{1/2}(\lambda_2+w\cos\theta)}\Bigg]\frac{\cos\frac{1}{2}\theta}{4(\lambda_1-\lambda_2)(\beta_\infty^{-4}+k_n^2)}, \end{aligned} \tag{C 4}$$

the constants C_{1-4} are given by

$$\left.\begin{aligned} C_1 &= \mathrm{i}2^{3/2}\left(\frac{A_t^*}{\beta_\infty^3} - k_nA_N\right), \quad & C_2 &= \mathrm{i}2^{3/2}\left(\frac{k_nA_t^*}{\beta_\infty} + \beta_\infty^{-2}A_N\right), \\ C_3 &= -\frac{\sqrt{2}A_t^*M_\infty^2}{\beta_\infty^3}, & C_4 &= -\frac{\sqrt{2}A_nM_\infty^2}{\beta_\infty^2}, \end{aligned}\right\} \tag{C 5}$$

the functions $f_{1,2}(\lambda)$ are defined by

$$\left.\begin{aligned} f_1(\lambda) &= [\mathrm{i}C_2 - 2C_4(\lambda+\beta_\infty^{-2})](-\beta_\infty^{-4}+k_n^2-w^2-2\beta_\infty^{-2}\lambda) \\ &\quad +[C_1+2\mathrm{i}C_3(\lambda+\beta_\infty^{-2})]2\mathrm{i}k_n(\lambda+\beta_\infty^{-2}), \\ f_2(\lambda) &= [\mathrm{i}C_2 - 2C_4(\lambda+\beta_\infty^{-2})]2\mathrm{i}k_n(\lambda+\beta_\infty^{-2}) \\ &\quad +[C_1+2\mathrm{i}C_3(\lambda+\beta_\infty^{-2})](-\beta_\infty^{-4}+k_n^2-w^2-2\beta_\infty^{-2}\lambda), \end{aligned}\right\} \tag{C 6}$$

and

$$\lambda_{1,2} = -\frac{\beta_\infty^{-2}}{2}\left[\frac{\beta_\infty^{-4}+k_n^2+w^2}{\beta_\infty^{-4}+k_n^2}\right] \pm \frac{\mathrm{i}k_n}{2}\left[\frac{\beta_\infty^{-4}+k_n^2-w^2}{\beta_\infty^{-4}+k_n^2}\right], \tag{C 7}$$

and it should be noted that the square roots in the above expressions are to be evaluated by introducing branch cuts joining $-\beta_\infty^{-2}$ and $-w$ to infinity through the lower half-plane, and joining $-\beta_\infty^{-2'}$ and w to infinity through the upper half-plane (see Myers & Kerschen 1995 for full details). Finally, we have

$$\begin{aligned} D_3(\theta) &= \frac{\mathrm{i}A_N}{[w(\beta_\infty^{-2}-w\cos\theta)]^{1/2}}\left[1-\frac{M_\infty^2}{\beta_\infty^2}-\frac{\beta_\infty^{-2}}{\beta_\infty^{-2}-w\cos\theta}\right] \\ &\quad +\frac{\mathrm{i}A_N(\gamma+1)M_\infty^4}{w^{3/2}(\beta_\infty^{-2}+w)^{1/2}\beta_\infty^4}\left[\frac{\beta_\infty^{-2}}{2}\cos\theta-\frac{w}{4}\cos 2\theta\right]. \end{aligned} \tag{C 8}$$

REFERENCES

Atassi, H. M., Subramaniam, S. & Scott, J. R. 1990 Acoustic radiation from lifting airfoils in compressible subsonic flow. *AIAA Paper* 90-3911.

Chapman, C. J. 1994 Sound radiation from a cylindrical duct. Part 1. Ray structure of the duct modes and of the external field. *J. Fluid Mech.* **281**, 293–311.

Envia, E. & Kerschen, E. J. 1986 Noise generation by convected gusts interacting with swept airfoil cascades. *AIAA Paper* 86-1872.

Fang, J. & Atassi, H. M. 1993 Compressible flows with vortical disturbances around a cascade of loaded airfoils. In *Proc. Sixth Intl Symp. on Unsteady Aerodynamics, Aeroacoustics and Aeroelasticity of Turbomachines and Propellers, Notre Dame, IN September 1991* (ed. H. M. Atassi) Springer.

Goldstein, M. E. 1976 *Aeroacoustics*. McGraw-Hill.

Goldstein, M. E. 1978 Unsteady vortical and entropic disturbances of potential flows round arbitrary obstacles. *J. Fluid Mech.* **89**, 433–468.

Jones, D. S. 1966 *Generalised Functions*. McGraw-Hill.

Kerschen, E. J. & Balsa, T. F. 1981 Transformation of the equation governing disturbances of a two-dimensional compressible flow. *AIAA J.* **19**, 1367–1370.

Kerschen, E. J. & Myers, M. R. 1986 Perfect gas effects in compressible rapid distortion theory. *AIAA J.* **25**, 504–507.

Kerschen, E. J. & Myers, M. R. 1987 A parametric study of mean loading effects on airfoil gust interaction noise. *AIAA Paper* 87-2677.

Koch, W. 1971 On the transmission of sound waves through a blade row. *J. Sound Vib.* **18**, 111–128.

Lee, S. W. 1978 Path integrals for solving some electromagnetic edge diffraction problems. *J. Math. Phys.* **19**, 1414–1422.

Myers, M. R. & Kerschen, E. J. 1984 Effect of airfoil mean loading on convected gust interaction noise. *AIAA Paper* 84-2324.

Myers, M. R. & Kerschen, E. J. 1995 Influence of incidence angle on sound generation by airfoils interacting with high-frequency gusts. *J. Fluid Mech.* **292**, 271–304.

Noble, D. 1988 *Methods Based on the Wiener–Hopf Technique*. Chelsea.

Peake, N. 1992 The interaction between a high-frequency gust and a blade row. *J. Fluid Mech.* **241**, 261–289.

Peake, N. 1993 The scattering of vorticity waves by an infinite cascade of flat plates in subsonic flow. *Wave Motion* **18**, 255–271.

Peake, N. & Kerschen, E. J. 1995*a* A uniform asymptotic approximation for high-frequency unsteady cascade flow. *Proc. R. Soc. Lond.* A **449**, 177–186.

Peake, N. & Kerschen, E. J. 1995*b* A parametric study of noise generation by a blade row with mean loading. *CEAS/AIAA Aeroacoustic Conference, June 1995, Munich.*

Robinson, A. & Laurmann, J. A. 1956 *Wing Theory*. Cambridge University Press.

Scott, J. R. & Atassi, H. M. 1990 Numerical solution of the linearized Euler equations for unsteady vortical flows around lifting airfoils. *AIAA Paper* 90-0694.

Smith, S. N. 1972 Discrete frequency sound generation in axial flow turbomachines. *Brit. Aeronaut. Res. Coun. R&M* 3709.

Thwaites, B. 1960 *Incompressible Aerodynamics*. Dover.

Verdon, J. M. 1993 Review of unsteady aerodynamic methods for turbomachinery aeroelastic and aeroacoustic applications. *AIAA J.* **31**, 235–250.

Whitehead, D. 1987 Classical two-dimensional methods. In *Axial-Flow Turbomachines, Volume 1: Unsteady Turbomachinery Aerodynamics* (ed. M. F. Platzer & F. O. Carta). *AGARD-AG*-298 Vol 1.

Woods, L. C. 1961 *The Theory of Plane Subsonic Flow*. Cambridge University Press.